Advancing Post-Combustion CO_2 Capture through Increased Mass Transfer and Lower Degradation

Final Technical Report

Work Performed Under Agreement Number
DE-FE0031661

Submitted by
The University of Kentucky Research Foundation
on behalf of the University of Kentucky Center for Applied Energy Research
2450 Research Park Drive
Lexington, KY40511

Principal Authors:
Jesse Thompson, Moushumi Sarma, Min Xiao, Saloni Bhatnagar, Keemia Abad and Kunlei Liu

Principal Investigator (PI)
Jesse Thompson Ph.D
Phone: (859) 257-0355
Fax: (859) 257-0220
Email: jesse.thompson@uky.edu

Report Issued
December 23, 2022

Submitted to
U.S. Department of Energy National Energy Technology Laboratory

U.S. DOE NETL Project Manager
Krista Hill
krista.hill@netl.doe.gov

ACKNOWLEDGEMENT: The University of Kentucky and the Lawrence Livermore National Laboratory are grateful to the U.S. Department of Energy National Energy Technology Laboratory for the support of this project.

Abstract:

The over-arching goal of the proposed project is to develop three techniques to enable aqueous post-combustion CO_2 capture technologies to meet the DOE performance and cost targets of 90% CO_2 capture, 95% purity, at a cost of less than $30/tonne CO_2 captured. This will be accomplished by the development of materials and processes to increase mass transfer in the absorber and reduce the environmental impacts. While constantly working to reduce the cost of CO_2 capture via solvent development and process & heat integration, increasing CO_2 mass transfer through development of custom dynamic packing materials and tuning solvent physical properties may offer a route to increased solvent capacity, lower energy consumption and reduced aerosol formation. The environmental concerns that have been identified in amine-based CO_2 capture systems, nitrosamines specifically, are another critical element that will be addressed in this project.

The specific objectives of the project were to: 1) conduct detailed studies to understand how solvent physical properties and aerosol formation are impacted by additives; 2) quantify the CO_2 mass transfer improvement from the dynamic polarity packing in the absorber and the additive-modified solvent using the existing UK bench-scale CO_2 capture unit; 3) quantify the energy consumption savings associated with enhanced mass transfer; 4) quantify the benefits of the UK's electrochemical cell to decompose nitrosamines; and 5) collect the necessary information/data to conduct a high-level TEA assessment of the proposed technologies.

The project involved the fabrication and installation of customized dynamic polarity packing and an investigation into the understanding of the impact of chemical additives on solvent properties to increase CO_2 mass transfer in the absorber column, and lastly the design of an electrochemical cell to decompose nitrosamines in a water wash. After both systems were fabricated, they were tested at UK facilities, including on the bench-scale CO_2 capture unit under parametric and long-term operation.

List of Acronyms

Acronym	Definition
2A1P	2-amino-1-amino-propanol
2EAE	2-(Ethylamino)ethanol
AMP	2-methyl-2-amino-propanol
ABS	Acrylonitrile Butadiene Styrene
ASTM	American Society for Testing and Materials
CFD	Computational fluid dynamics
C/N	Carbon to nitrogen ratio
CO2	Carbon dioxide
CCS	Carbon Capture System
DEA	Diethanolamine
CX	Carbon Xerogel
DMEA	Dimethylethanolamine
DOE	Department of Energy
DP	Dynamic Packing
E-cell	Electrochemical cell
EDA	Ethylenediamine
HDA	Hexanediamine
HDPS/HIPS	High density polystyrene / High impact polystyrene
L/G	Liquid to gas ratio
LLNL	Lawrence Livermore National Laboratory
LOD	Limit of detection
MDEA	Methyldiethanolamine
MEA	Monoethanolamine
NDEA	Nitrosodiethylamine
NETL	National Energy Technology Laboratory
NMEA	N-Methylethanolamine
NMOR	Nitrosomorpholine
NPY	Nitrosopyrrolidine
PCC	Post combustion CO_2 Capture
PLA	Polylactic acid
PZ	Piperazine
SEM	Scanning electron microscope
SS	Stainless steel
TEA	Techno-economic Assessment
UK	University of Kentucky
WWC	Wetted Wall Column

1.) Executive Summary

With funding from the U.S. Department of Energy (DOE), the University of Kentucky (UK), with collaboration from Lawrence Livermore National Laboratory (LLNL) designed, fabricated, and tested customized dynamic polarity packing to increase CO_2 mass transfer in the absorber column. The impact of chemical additives on solvent physical properties to increase solvent wetting on the packing was also investigated. Lastly, an electrochemical process was constructed to decompose nitrosamines from the water wash.

UK has worked with LLNL on the design and 3D printing of dynamic packing that have been co-printed with two different polymers with different contact angles (polarity) relative to an aqueous amine solvent. As the solvent moves down the packing it will relatively wet or coat the polymer material that is less hydrophobic, then as it contacts the more hydrophobic polymer the solvent will wick-up away from the hydrophobic polymer section. The solvent will then re-wet as it re-contacts the more hydrophilic base packing material. This process will create turbulence and inter-solution mixing within the solvent which can reduce CO_2 diffusion resistance and increase overall mass transfer. The first step in the development of this concept was to identify several polymers with different contact angles relative to the amine solvent and verify that these polymers are stable (no change in mass, shape, or contact angle) in CO_2-loaded amine solvent at relatively high temperatures (absorber bulge temperature, 60-70 ^oC). Acrylonitrile butadiene styrene (ABS), Nylon, and high-impact polystyrene (HIPS) polymers were verified to be stable (> 5000 hours).

Several different packing designs were fabricated and tested along with the baseline stainless steel packing. The steel packing and all the 3D printing packings were in the 250Y geometry. Generally, all the 3D printed polymer packings exhibited improvements in CO_2 absorption performance when compared to the conventional steel packing. The same CO_2 absorption efficiency can be achieved with higher CO_2 loading in lean return solvent, and the CO_2 loading of rich solvent is shifted to a higher loading region. This also translates to reduction in energy demand in the stripper at same CO_2 absorption efficiency.

The long-term packing verification testing of a Nylon/HIPS 3D printed polymer packing consisted of 500 hours of stable CO_2 capture under optimal conditions. The polymer packing shows a consistent improvement in mass transfer leading to an average CO_2 absorption of 60.1% and energy demand of 233.8 kJ/mol CO_2. Overall, this translated to a relative 15.9% improvement in CO_2 absorption and 19.7% decrease in energy consumption compared the baseline 250Y stainless steel packing.

These two absorber configurations showed similar CO_2 absorption rate and demonstrated that mass transfer in the absorber column was enhanced with the more efficient dynamic packing and can reach the CO_2 removal target with less packing height (66.7% of original height). By reducing the required amount of packing the size of the absorber column and its capital expense can be substantially reduced. After the 500-hour testing period, a detailed solvent degradation analysis was conducted. The total solvent degradation matched with previous testing campaigns using the same solvent at bench and pilot scales. No new degradation products were identified in the solvent with the polymeric packing and suggested that the polymer packing has minimal to no impact on solvent stability.

A TEA report was generated and summarizes the evaluation of a CO_2 capture technology developed by University of Kentucky (UK) for post-combustion carbon capture. The evaluation uses a TEA report prepared by Trimeric Corporation as the basis for the UK CO_2 capture process with UK amine solvent. A process modification was added by applying advanced packings in the absorber to enhance mass transfer and decrease the absorber size using the UK amine solvent CO_2 capture system. This assessment assumed that the cost of the absorber packing is the same for steel and the 3D printed polymers with the decrease in capital cost only related to decreasing the size of the absorber and it ancillary impact on the CO_2 capture system. The UK process with advanced packings shows reduction in levelized cost of electricity (~10.4%), and cost of CO_2 capture (~24.4%).

Lastly, this project successfully developed a process to neutralize nitrosamines derived from amine solvents using an electrochemical treatment. Nitrosamines (as a class of compounds) can be decomposed through an electron transfer to re-form a secondary amine. Initially a small electrochemical cell was prepared using a UK-developed carbon electrode material. The characterization of the electrode material was performed, followed by nitrosamine decomposition testing to determine the mechanism of decomposition, and calculated the efficiency of the process. General operating parameters of the electrochemical cell were identified. At the optimized operating conditions the concentrations of three nitrosamines reached our LOD within 12 hours with a 99% removal efficiency.

2.) Introduction, Background and Technology Description

Physical Properties of Amine Solvents

A limited number of amine compounds are available for CO_2 capture after balancing the capital cost and energy penalty of these aqueous amine-based solvents. In the carbon capture process, physical properties such as viscosities and surface tensions are found to play an important role in solvent performance. These properties directly affect the wettability of the amine solvents on the packing material absorber column which in turn affect the CO_2 flux into the solvent (**Figure 1**). The physical aspects of absorption are dependent on the CO_2 concentration (partial pressure), the amine concentration, and localized mixing that can assist in overcoming mass transfer resistance. The physical properties such as viscosity and surface tension will impact the contact angle of the solvent on a particular packing material surface used in the absorber column and are mainly responsible for solvent wettability and gas−liquid effective interfacial area. In the absorber, depending on the details of the process, absorbent solutions with different surface tensions can be favored. For example, low surface tension solvents are desirable for packed columns while high surface tension solvents are preferred for membrane-based absorbers to avoid unfavorable wetting phenomena.

- $flux = A \cdot k_G \cdot (P^g_{CO_2} - P^*_{CO_2})$

$$\text{Where } k_G \propto \frac{\sqrt{D_{CO_2} \cdot k_2 \cdot [amine]}}{H_{CO_2}}$$

Figure 1. Equation for the calculation of CO_2 flux into an amine solvent.

It can be expected that amine solvents with a high kinetic rate constant would see a proportionally similar mass flux, but this is not observed. An example of this phenomenon is presented in **Figure 2** comparing three different amine solvents: monoethanolamine amine (MEA), piperazine (PZ), and methyldiethanolamine (MDEA). The rate constant for MDEA is orders of magnitude slower than for MEA and PZ but the measured mass flux (by Wetted Wall Column - WCC) is only marginally lower. The relatively slow CO_2 mass flux for the PZ and MEA solvents can be related to the physical properties of these solvents creating some additional mass transfer resistance.

The physical properties of amine solvents can also be impacted by additives used to control operational issues such as foaming, corrosion, or to mitigate oxidative degradation through O_2 scavenging. All advanced amine solvents are generally accepted to contain some additives to address some or all of these operational concerns. However, the specific impact of these additives on the physical properties, and consequently on mass transfer resistance, is not well understood.

Generally, the physical properties commonly used primary, secondary, tertiary and diamine solvents with comparable alkalinities and variable carbon loadings are not well studied. Therefore, this study enables us to understand physical properties and their relationship to solvent flow and wettability inside the absorber column, especially at the bottom where the CO_2 loading is highest, but mass transfer is limited.

	MEA	PZ	MDEA
Rate Constant	5.94	69.21	0.004
Self-concentrated amine	1.0	3.5	~1
Calculated Kg' impact from [M]	1	1.87	~1
Calculated Kg' impact from k_2	1	3.41	0.03
Calculated Kg' Overall	**1**	**6.39**	**0.03**
Measured Mass Flux (WCC@0.1)	1	2.20	0.18

Figure 2. Examples of measured CO_2 flux from three different solvents with different kinetic rates.

Dynamic Packing using Polymers and 3D Printing

For the liquid-based CO_2 capture, the absorption happens in an absorber column using packing to provide a large interfacial area for efficient mass transfer. Structured packing is widely used to handle the large gas volume with low gas-side resistance. These packing can guide the solvent through a designated path for low-pressure drop and less liquid holdup. Many different packing designs have demonstrated that structured packings could provide a large effective interfacial surface to realize efficient CO_2 removal from flue gas. Although the dimension of the absorber column is significantly reduced because of the existing structured packings, it is still one of the largest and priciest devices in the purchased equipment for absorption-based CO_2 capture plant. In addition, many advanced absorbents have been proposed for low regeneration energy cost, but with a trade-off of higher viscosity. It is well known that increasing absorbent viscosity leads to lower diffusivity within the liquid phase, larger liquid holdup, and thicker liquid film, which means greater mass transfer resistance for CO_2 absorption. Some previous studies have suggested that mass transfer intensification for gas absorption in viscous absorbent can be impacted through stronger turbulence and better mixing effect within the liquid phase. However, these studies were carried out in the existing plate surface and the turbulence was realized through the mechanical modifications, which might decrease the surface area and increase the liquid holdup.

One approach to increase turbulence and better mixing effect within the liquid phase of the solvent involves flowing the solution over alternative surfaces with different relative hydrophobicity's (or hydrophilicity's). This novel dynamic polarity packing (DP packing) can be used to drive macro-scale turbulence hydraulically through a selected pattern. The in-situ manipulation of flow hydraulic through alternating the surface with relative hydrophilicity and hydrophobicity enables DP packing to entirely mimic the geometry of conventional packings without additional mechanical obstacles (**Figure 3**). This type of material can be fabricated through Additive Manufacturing, or 3D printing. This emerging fabrication technology allows for greater design freedom and the utilization of abundant alternative materials for customized prototypes.

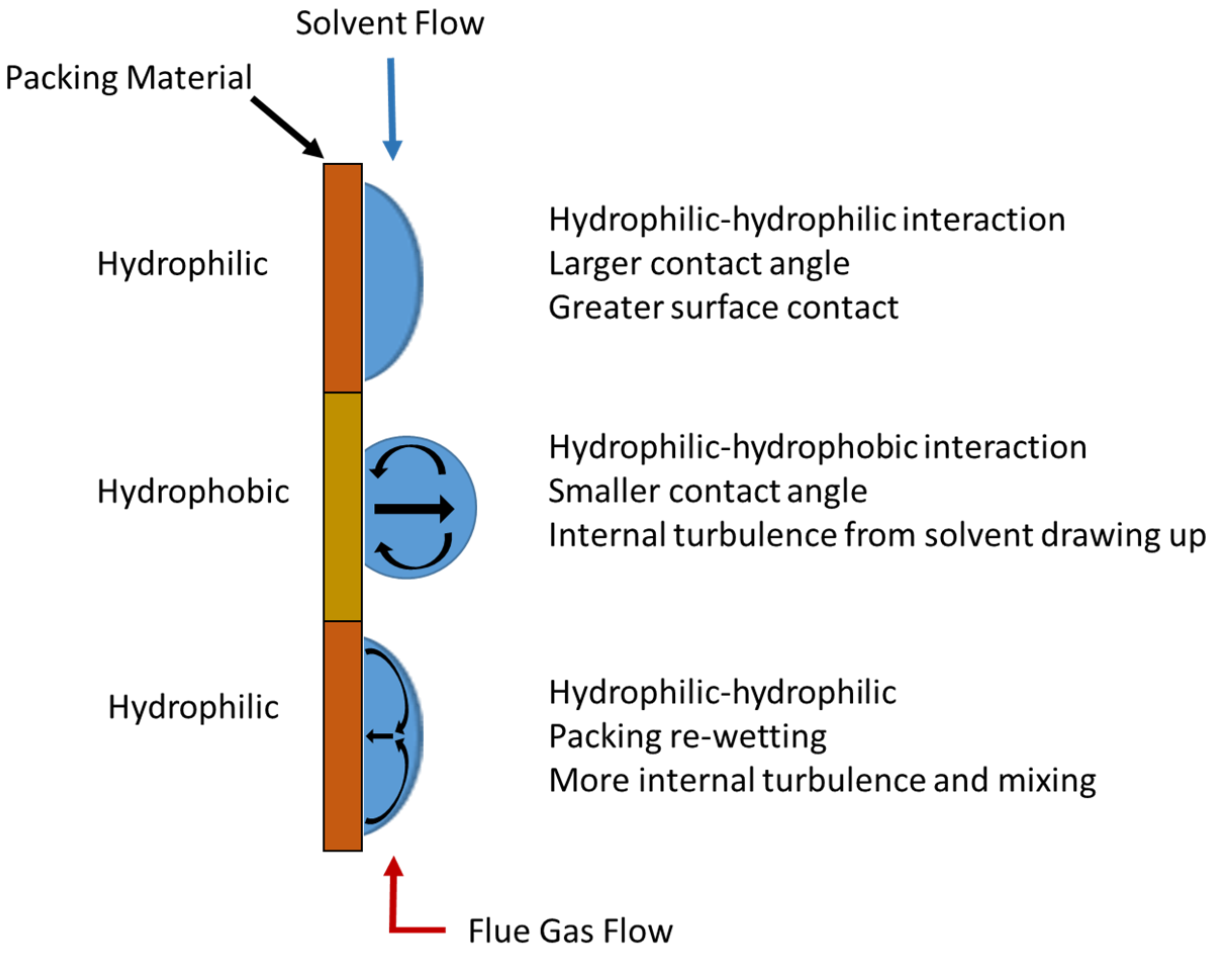

Figure 3. Conceptualization of macro-scale turbulence generated hydraulically through alternating surfaces of relative hydrophilicity and hydrophobicity polymers.

Prior to this project, LLNL explored the potential benefit that might be achieved with alternating hydrophilic and hydrophobic polymer surfaces. **Figure 4** shows an amine solution flowing down a hydrophilic plate imbedded with strips of hydrophilic polymeric material while CO_2 is passed over the solution. The amount of CO_2 absorbed by the solvent increased when the hydrophobic patches were added to the hydrophilic surface due to the increase in liquid turbulence. Newer 3D printers are capable of printing with two different polymers within the same print, known as co-printing, to generate these types of patterns. Optimization of this macro-scale turbulent mixing can be achieved through different patterns and through differences in the magnitude of the hydrophilic/hydrophobic surfaces as measured through contact angle measurements. Additionally, the stability of the polymers upon exposure to specific amine solvents will need to be examined to identify polymers that can withstand the high pH and temperature conditions within the absorber column.

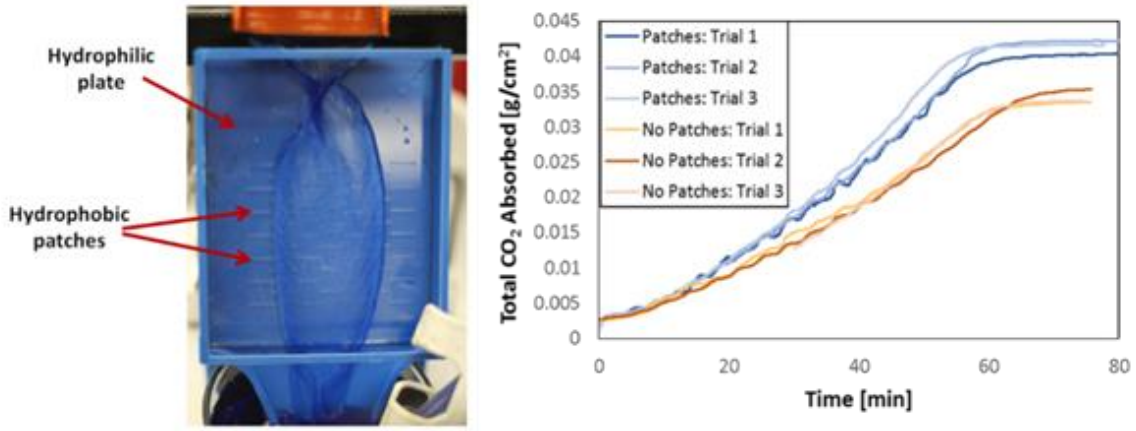

Figure 4. Amine solution flowing down a hydrophilic plate imbedded with strips of hydrophilic polymeric material while CO_2 is passed over the solution showing an increase in CO2 absorption when the hydrophobic patches are present.

Nitrosamines in CO_2 Capture

Significant challenges exist in controlling the emissions of hazardous amine degradation products, including carcinogenic N-nitrosamines, from post-combustion carbon capture systems. N-nitrosamine compounds can form from secondary amine solvents or degradation compounds and accumulate in the amine solvent loop and waterwash sections prior to being emitted into the atmosphere. Due to the recent rapid development of CO_2 capture systems employing aqueous amine solvents, N-nitrosamines now represent an emerging environmental concern if their formation and emission from CO_2 capture systems cannot be better understood and controlled.

Some current wastewater treatment methods have been assessed and applied to CCS systems with limited success. The relative complexity and/or cost of these N-nitrosamine mitigation strategies may make implementation on a large industrial scale cost prohibitive, requiring simpler and more cost-effective approaches to be developed. Currently, CCS waterwash systems are the last location where nitrosamine can be captured prior to emission and the Henry's volatility coefficients of these N-nitrosamines from water suggests that water wash systems can be effective at capturing the N-nitrosamines. These systems circulate water in a closed loop, with occasional blowdown to either the amine loop (to recover amine) or to an external water treatment system within the power plant.

N-nitrosamines can be effectively removed from water through a variety of treatment options including biological treatments, adsorption onto activated carbons (based on the N-nitrosamine hydrophobicity), using filtration membranes (micro, ultra and nanofiltration), and reverse osmosis and ultraviolet treatments. Another removal option is to use carbon materials as sorbents. Liu et al. (2016) studied the use of a capacitive deionization cell containing carbon electrodes to remove organic disinfection byproducts from wastewater (*Sci. Total Environ. 568, 19–25. https://doi.org/10.1016/j.scitotenv.2016.05.219*). In this process, the organic compounds are physically adsorbed onto the carbon electrode surface due to their relative affinity (polarity). The adsorbed organic compounds were then electrochemically oxidized from the electrode surface using an applied potential. This type of process can decompose hazardous compounds without the need for additional steps or the production of undesired byproducts. Expanding on this concept,

this project proposes the development and testing of an electrochemical process using stationary carbon electrodes inside an electrochemical cell to adsorb N-nitrosamines from an aqueous solution followed by electrochemically mediated reduction of N-nitrosamines from CCS waterwash solutions (**Figure 5**).

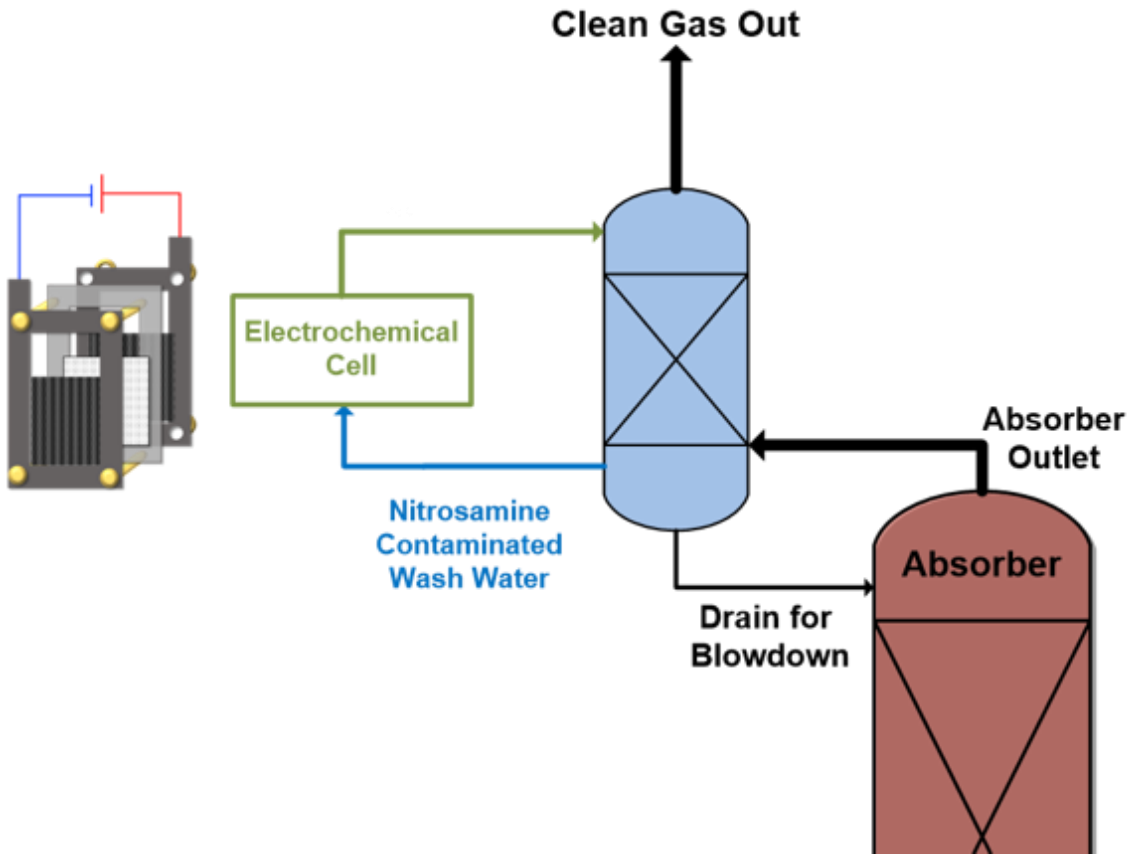

Figure 5. Electrochemical cell to adsorb N-nitrosamines from an aqueous solution followed by electrochemically mediated reduction of N-nitrosamines from CCS waterwash solutions.

Preliminary experiments showed that electrochemical reduction of nitrosamines is viable. A simple lab-scale electrochemical cell with a carbon electrode, a titanium counter electrode, and stir bar for agitating the N-nitrosamine solution was assembled (**Figure 6**). Solutions of nitrosodiethylamine (NDEA) and nitrosopyrrolidine (NPY) at a concentration of 100 mg/L (each), with 1% monoethanolamine were prepared and sparged with CO_2 to simulate possible waterwash solutions containing both amines and N-nitrosamines. Decomposition of both nitrosamines from the simulated CCS waterwash solution was achieved up to 92% for NPY and 82% for NDEA at 300 mA for 1 h in **Figure 7** (*Int J Greenhouse Gas Control 83 (2019) 83–90. https://doi.org/10.1016/j.ijggc.2019.02.003*). This concept was further optimized and tested through fabrication of flow-through electrochemical cell to increase nitrosamine removal and increase energy efficiency followed by evaluation using authentic waterwash collected at a Small Pilot CCS.

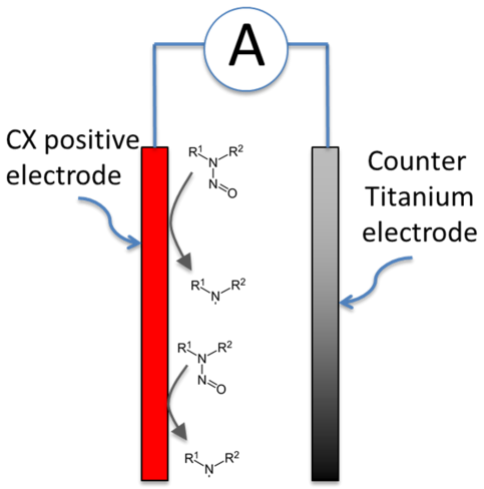

Figure 6. Simple lab-scale electrochemical cell with carbon xerogel (CX) electrode, titanium counter electrode, and stir bar for agitating the N-nitrosamine solution.

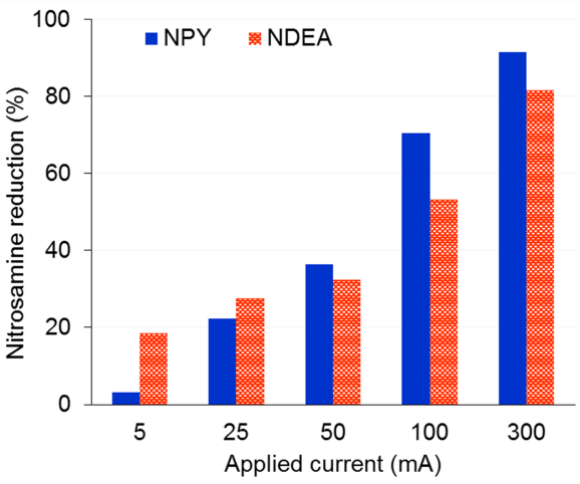

Figure 7. Nitrosamine decomposition from the simulated CCS waterwash solution at 300 mA applied current for 1 hour in a simple electrochemical cell (*Int J Greenhouse Gas Control 83 (2019) 83–90*).

3.) Project Technical Results

3.1 Investigation of Solvent Physical Properties with Additives (Task 2)

A systematic approach was taken to develop a better understanding of the structure/function relationships for amine solvents in terms of physical properties and how they can be applied to better understand bubble formation, the stability of gas-liquid interface film and solvent polarity. Physical properties including density, dynamitic and kinematic viscosity, surface tension, and contact angle (versus a polymeric ABS surface) were measured of commercially available amines (as aqueous solvents) with different pKa, polarity and functional groups (i.e. –OH, -N, -R). The impact of solvent additives on physical properties was also explored with a focus on identifying additive(s) that can increase solvent wetting on packing material surface by decreasing surface tension and contact angle (versus the packing surface).

The key accomplishments were developing the understanding that solvent contact angle (wettability) is directly related to the surface tension of the solvent, and that the addition of a surfactant-type additive in less than 0.1% concentrations can significantly decrease surface tension of every amine solvent examined. A commercially available surfactant additive was able to exceed our target value (milestone) by modifying the surface tension of these amine solvents by > 20%, while also yielding a corresponding decrease in the contact angle (wetting) of these solvent against a polymer surface.

3.1.1 Physical Property Measurements for Amine Solvent

Commercially available amines, including primary, secondary, tertiary amines, and diamines with different functional groups were prepared at various concentrations (e.g., 3, 5 M) and at lean (~

0.2 carbon/nitrogen (C/N) ratio) and rich carbon loadings (~ 0.4 C/N). Physical properties including density, dynamitic and kinematic viscosity, surface tension, and contact angle (versus a polymeric ABS surface) were measured of commonly available amines (as aqueous solvents) with different pKa, polarity and functional groups (i.e. –OH, -N, -R). One amine included in the original set, tertiary triethanolamine, had a very high viscosity with CO_2 loading of approximately 20 cP. This level is outside of the UK target for aqueous amines (less than 15 cP). Given the high viscosity level, this amine was excluded from future physical property measurements. Likewise, 2-methyl-2-amino-propanol (AMP) as a single amine solvent precipitated above the typical lean-loading range and was also excluded from further physical property assessments. This left a set of 11 representative amines to be evaluated in the full physical property measurement study.

All the measured physical properties changed relative to an increase in CO_2-loading. As expected, solution density and viscosity both increased by small percentage as the solvent adsorbed CO_2. More interesting was the observed increases in surface tension as CO_2 was loaded into the solvent (**Figure 8**) among all the different types of amines including primary, secondary, diamines and tertiary amines. The implication of this trend is that the solvent (amine+water) shifts its surface properties closer to those of water, which has a surface tension of just above 70 mN/m (@ 20 °C), as it absorbs CO_2 This change also applies to the measured contact angles of these solvents relative to a hydrophobic polymeric surface such as ABS, as the contact angles also increased along with CO_2-loading (**Figure 9**). This suggests that the amine solvent is transitioning from a more non-polar solution to a more polar solution (water-like) as it absorbs CO_2. When translated to polymeric packing, this suggests less wetting on the packing surface as CO_2 loading increases as the solvent moves down the absorber column.

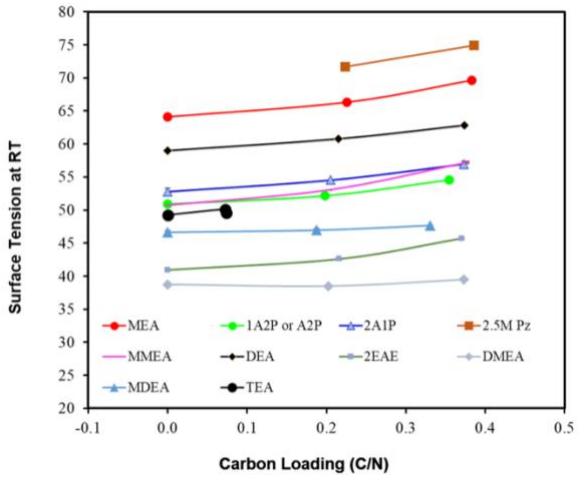

Figure 8. Measured surface tension (mN/m) of amine solvents as a function of CO_2-loading.

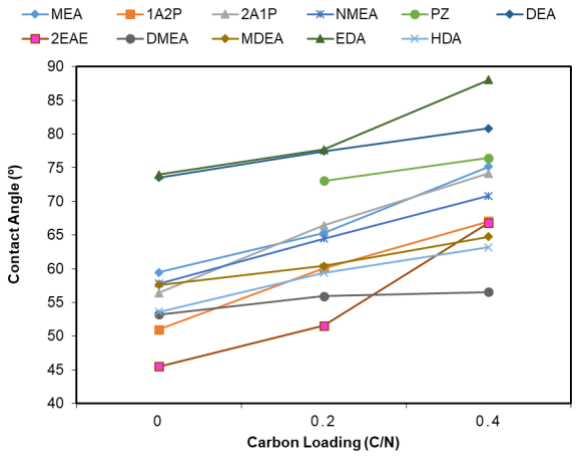

Figure 9. Measured contact angle (°) of amine solvents as a function of CO_2-loading (versus a polymeric ABS surface)

3.1.2 Predictive Solvent Property Model Development

A general assessment of the physical properties of aqueous amine solvents was conducted based on their chemical properties including molecular structure, pKa, polarity and electron density of

amines. Each amine was evaluated based on a relative scale (1-5) of each physical property from low to high within the set of amines. The model/assessment was constructed by regressing the scaled/normalized measured physical and fundamental chemical parameters. This allowed the impact on mass transfer from physical properties (surface tension, elasticity, etc.) to be estimated based on the molecular structure of the amine.

Three interesting results from this were; (1) the viscosity and surface tension of the solvent (with CO_2-loading) is positively related to the molecular weight of amine (higher molecular weight corresponds higher viscosity), (2) the surface tension and contact angle can be related to the electron density around the active nitrogen (Millikan charge), (3) the contact angle is related to the hydrophobicity (log p) of the amine, (4) and the surface tension can be related to the pKa of the amine.

Figure 10 shows several different relations inferred between surface tensions and viscosities at zero carbon loadings for 5M alkalinity of the different amines. Surface tension and viscosity are inversely proportional (**Figure 10a**). **Figure 10b** shows that contact angles (on ABS surface) of a solvent increase along with surface tension. This indicates solvents with lower surface tensions wets the surface of the ABS polymer better. Lastly, **Figure 10c**, shows as the viscosity increases the contact angle decreases with a few abnormalities.

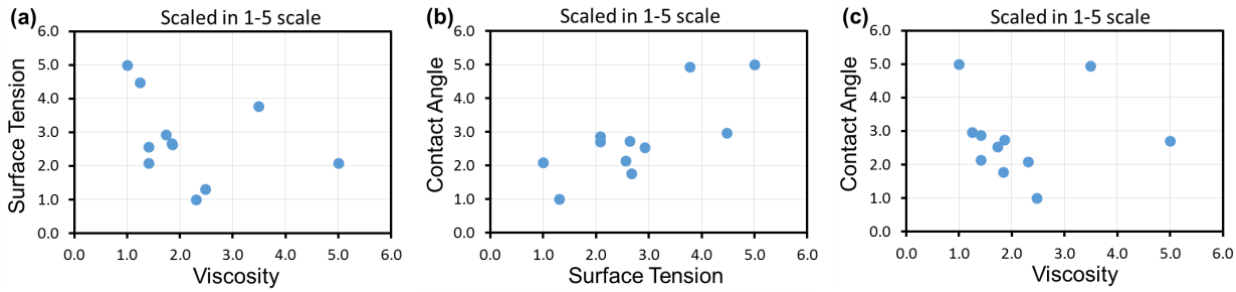

Figure 10: Relation between selected physical properties of different amines at zero carbon loading.

Figure 11a shows the relation between amine Log P (K_{ow}) with surface tension at zero carbon loadings. A negative value for Log P(K_{ow}) means the compound has a higher affinity for the aqueous phase (it is more hydrophilic); when Log P(K_{ow}) = 0 the compound is equally partitioned between the lipid and aqueous phases; a positive value for Log P denotes a higher concentration in the lipid phase. So lower Log P(K_{ow}) means more hydrophilic amine in this case. The properties Log P (K_{ow}) and surface tensions are found to be inversely proportional to each other. **Figure 11b** shows increase of dynamic viscosities with increase in molecular weights with one or two abnormalities. **Figure 11c** shows the plot of contact angle vs Log P indicating inversely proportional relation between these two properties.

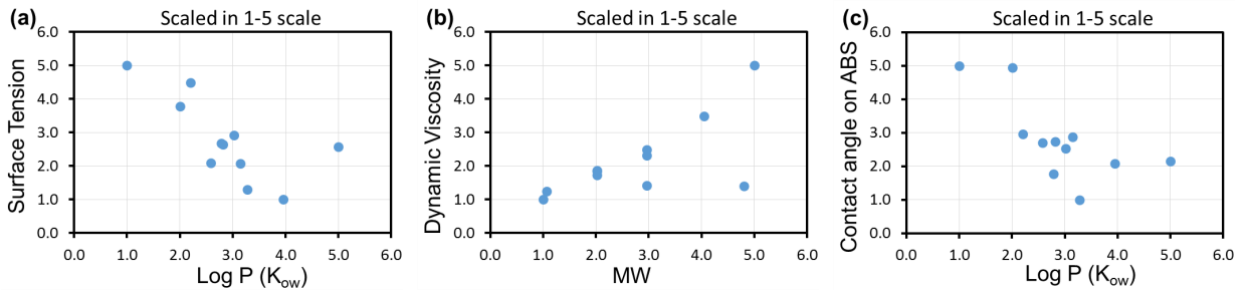

Figure 11: Relation between physical and chemical properties of different amines at zero carbon loading

3.1.3 Impact of Chemical Additive - Predictive Model Development

Chemical additives, commonly used in amine solvents, were selected with different functionality and chemical structures (halogenated surfactants, inorganic metal corrosion inhibitors, organic oxidation inhibitors, and metal-ligand catalyst). The selected additives were combined with the set of amine solvents and their physical properties, such as surface tension, viscosity, elasticity and contact angle of the blended solutions were re-measured. Changes in physical properties upon addition of the additive were examined. Additives that increase elasticity and decrease surface tension were of particular focus as they have the potential to increased CO_2 mass transfer and may increase compatibility (wetting) of the solvent with polymeric packing surfaces.

One compound was selected from each class of common additives including: oxidation inhibitor, corrosion inhibitor, surfactant, anti-foam agent, and catalyst. The selected compounds were: 2-Mercaptobenzothiazole – oxidation inhibitor; sodium metavanadate – corrosion inhibitor; surfactant; Xiameter – antifoam; C5c – CO_2 hydration catalyst. The physical properties were measured (density, kinematic and dynamic viscosity, surface tension, contact angle on ABS and surface elasticity) at lean and rich CO_2 loading containing the additives (oxidation inhibitor, corrosion inhibitors, surfactant, and anti-foam agent) to assess how the additives changed the solvent physical properties.

The trends generally are consistent within each group of similar solvent types (e.g., primary, secondary, tertiary and diamines). The only additive to have a significant impact on the physical properties of these solvents was the surfactant additive. The addition of the surfactant resulted in a decrease in surface tension and a measurable amount of surface elasticity (normal amine solvents do not have measurable surface elasticity). A 40% average decrease in surface tension was observed among primary amines after addition of surfactant to lean and rich CO_2-loaded solvents. A 32% average decrease in surface tension was observed among secondary amines after addition of surfactant to lean and rich CO_2-loaded solvents

A more concise way to look at the relevant physical property data is to plot the surface tension and contact angle of the amine solvents before and after the addition of the surfactant (**Figure 12**). From this plot, it is clear that the surfactant additive has decreased the surface tension of all the solvents, thereby also decreasing the contact angle and wettability of all of these solvents on packing surface. This result shows that the physical properties of amine solvents can be manipulated using a very small amount of an additive to increase wettability on packing surfaces.

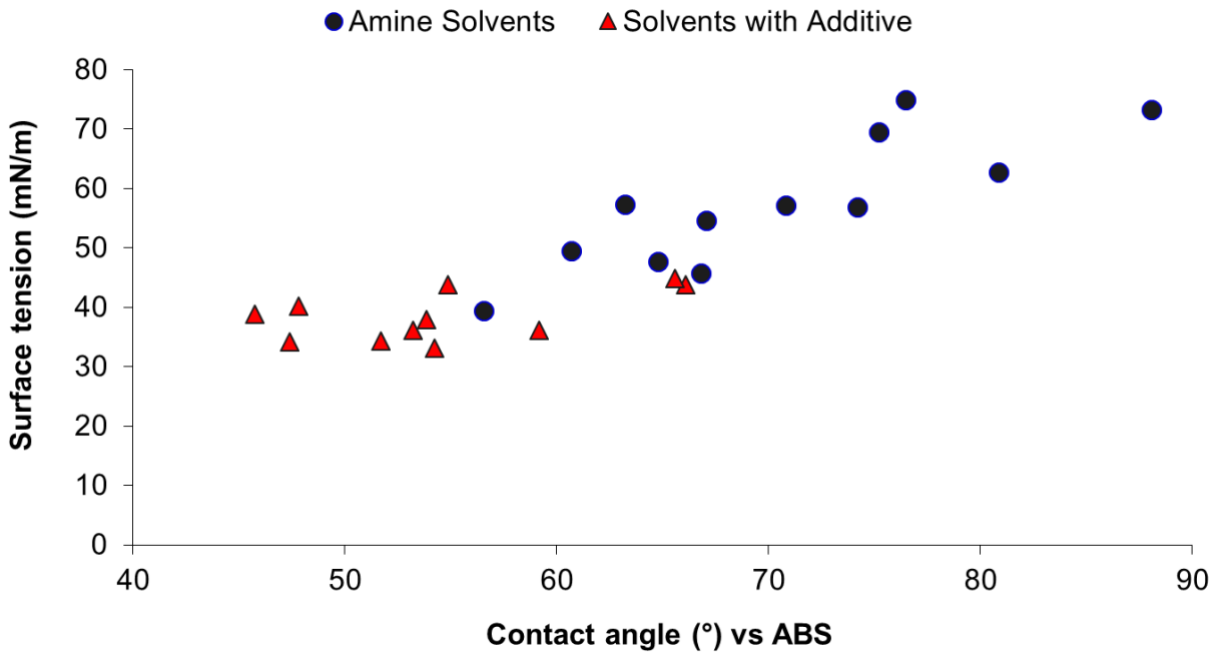

Figure 12. Modification of surface tension and contact angle (vs. ABS surface) upon the addition of a small amount (< 0.1%) of surfactant additive to eleven common amine solvents.

3.1.4 Solvent Properties and Bubble Formation

Four amines were down-selected from the original list of eleven from Task 2.1 based on criteria including: low viscosity (below 10 cP), commercial availability and cost (below ~$10 /kg), and no observed precipitation at rich CO_2-loading. Amine solvent solutions were prepared with lean-CO_2 loading and combined with the surfactant additive (identified in Subtask 2.3) for bubble formation and stability testing. An ASTM bubble column apparatus was assembled and used for these experiments. Increases in mass transfer as the result of bubble formation above liquid level will be measured in pH drop and breakthrough experiments.

The surfactant had no effect on viscosity and densities of the solutions, but the contact angle and surface tension of the amine solvent are all lower upon addition of these surfactant. As a surfactant, these classes of compounds contribute to micro-bubble formation under gas-low conditions. This micro-bubble formation will lower diffusion resistance and increase CO_2 mass transfer. The slope of the pH-drop during CO_2 saturation in a batch mode operation indicate the relative rate of CO_2 adsorption, which is faster when the solvent contains the surfactant compared to the baseline amine solvent (**Figure 13**). During the same experiment the CO_2 balance was monitored (CO_2 in and out of reactor) and the rate of CO_2 removal was calculated in the baseline and surfactant enhanced solvents (**Figure 14**).

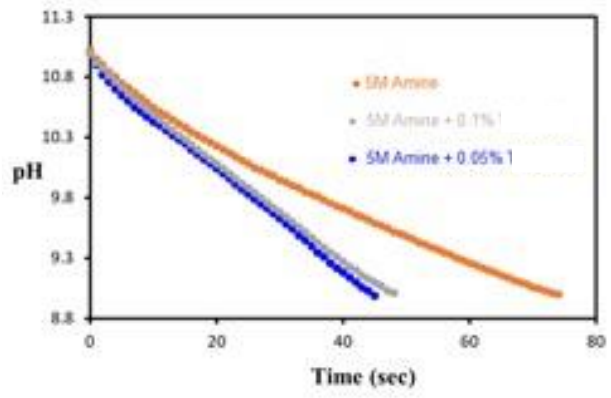

Figure 13. pH-drop of amine solvent baseline and with two different concentrations of surfactant additive.

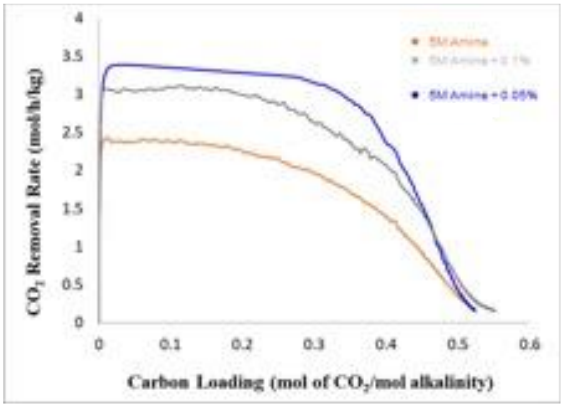

Figure 14. CO_2 breakthrough of amine solvent baseline and with two different concentrations of surfactant additive.

The CO_2 removal rate was also faster with the surfactant enhanced solvent. In terms of bubble formation, the solution with 0.05% surfactant produced small, less stable bubbles compared to the higher concentration (**Figure 15, 16**), with minimal difference in CO_2 adsorption rates. Other amine solvents, including secondary, tertiary and diamines, also show similar positive impacts on reducing CO_2 diffusion resistance through microbubble formation. This result shows that using a small amount of a surfactant gives the significant benefits in terms of lower CO_2 and amine diffusion resistance without generating overly stable bubbles. The additive was identified, through the work in this task, as the current best candidate to use in small bench testing.

Figure 15. At 0.1wt.%, the solution produces larger and relatively more stable bubbles upon saturation with CO_2.

Figure 16. At 0.05wt.%, the solution produces relatively smaller, less stable bubbles, but similar CO_2 adsorption rates.

3.1.5 Solvent Properties and Aerosol Formation, Corrosion, Degradation

Two common heat stable salts (as a proxy for solvent degradation) and commonly reported amine degradation products (acetate, formate, oxazolidine) were added to three representative amine solvents (down selected from the original list of eleven) at high concentration to determine their influence on the solvent physical properties. The viscosity of the primary, secondary and tertiary amine solvents increased in the solutions containing a mixture of different common degradation

compounds. This was expected and has been observed on both lab-scale and pilot solvent testing. However, the surface tension and contact angle of the primary, secondary and tertiary amine solvents were not meaningfully impacted by the addition of these common degradation compounds. This shows that in terms of the solvent physical properties related to wettability, specifically surface tension, there is a minimal impact from solvent degradation. No corrosion or deformation of the polymers were observed during longer term stability testing in rich CO_2-loaded solvents. The vapor pressure of all the additive examined was very low (low volatility), with low, to no, volatile emissions expected. This was verified during bench testing by collecting emission sample and analyzing for the additive and increases in amine emissions.

3.2 Development and Procurement of Dynamic Packing Material (Task 3)

UK has worked with LLNL on the design and initial printing of 3D dynamic packing material that have been co-printed with two different polymers with different contact angles (polarity) relative to the aqueous amine solvents. As the solvent moves down the packing it will relatively coat the polymer material that is less hydrophobic, then as it contacts the more hydrophobic polymer the solvent will wick-up away from the hydrophobic material. It will then re-coat as it contacts the more hydrophilic base packing material. This process will create turbulence and inter-solution mixing within the solvent which can be beneficial to reduce CO_2 and unreacted amine diffusion resistance and increase overall mass transfer. The first step in the development of this concept was to identify several polymers with different contact angles relative to the amine solvent and verify that these polymers are stable (no change in mass, shape, or contact angle) in CO_2-loaded amine solvent at relatively high temperatures (absorber bulge temperature, 60-70 ^oC). These polymers were verified to be stable (> 5000 hours) under the test conditions and meet the stability milestone; acrylonitrile butadiene styrene (ABS), nylon, and high-density polystyrene (HDPS). The contact angle differences of these polymers when measured against a representative CO_2-loaded amine solvent were generally greater than 20% and should produce the solvent turbulence necessary to reduce diffusion resistance and increase mass transfer. LLNL is printing the 3" dynamic packing sections to be installed at the UK small bench CO_2 capture unit.

3.2.1 Design Specifications

The dimension and characteristic for the packing under study is to simulate the general design of Mellapak 250Y using 3D printing with polymer materials co-printed with a pattern of more hydrophobic material over a relatively more hydrophilic base material. The first step was to identify polymer stable in CO_2-amine solvents that can be 3D printed by LLNL. Small coupons of the polymer candidates were printed and shipped to UK for stability assessment with the amine solvents. Based on the amine stability studies (Subtask 3.2), polymeric materials ABS, Nylon and HDPS (also called HIPS) were identified that were stable upon exposure to CO_2-loaded amine solvent at anticipated absorber temperatures.

Figure 17. Polished ABS coupon used as the base for contact angle (θ) measurements.

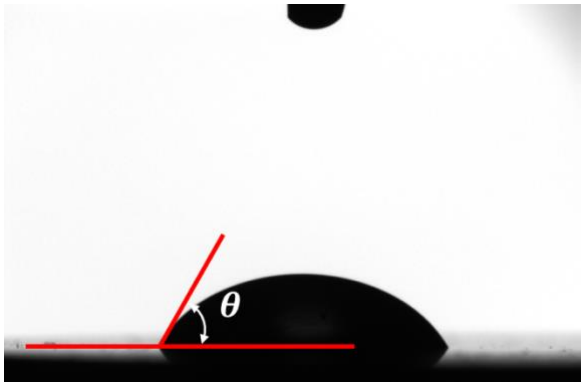

Figure 18. Contact angle (θ) on ABS surface with solution of 5M MEA (CO_2-loading of 0.2 C/N).

The next step was to measure the relative contact angle of these materials. The coupons were polished to use as the plate surface (**Figure 17**) for contact angle (θ) measurements using an Optical Tensiometer (**Figure 18**). Their contact angles were measured with water (**Figure 19)** and an amine solution at different carbon loadings (**Figure 20)**. The contact angle of water and the amine solvent relative to these polymeric surfaces is higher when compared to stainless steel (SS) due to the relative hydrophobicity of these polymers. Most interesting was the increase in contact angle (wettability) with CO_2-loading on all the packing surfaces. Overall, the contact angle of Nylon was the closest to SS, with both ABS and HDPS having 2-3 times larger contact angles. Based on this, the current best polymer for the base packing material is Nylon, augmented with ABS or HDPS used for the hydrophobic enhanced sections.

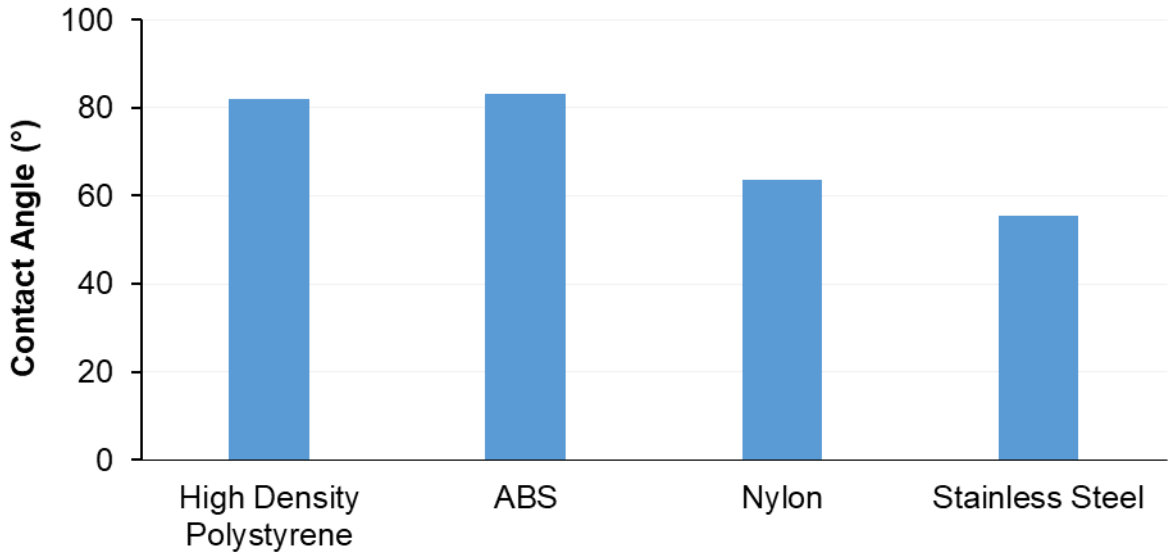

Figure 19. Contact angle of water on different packing material surfaces.

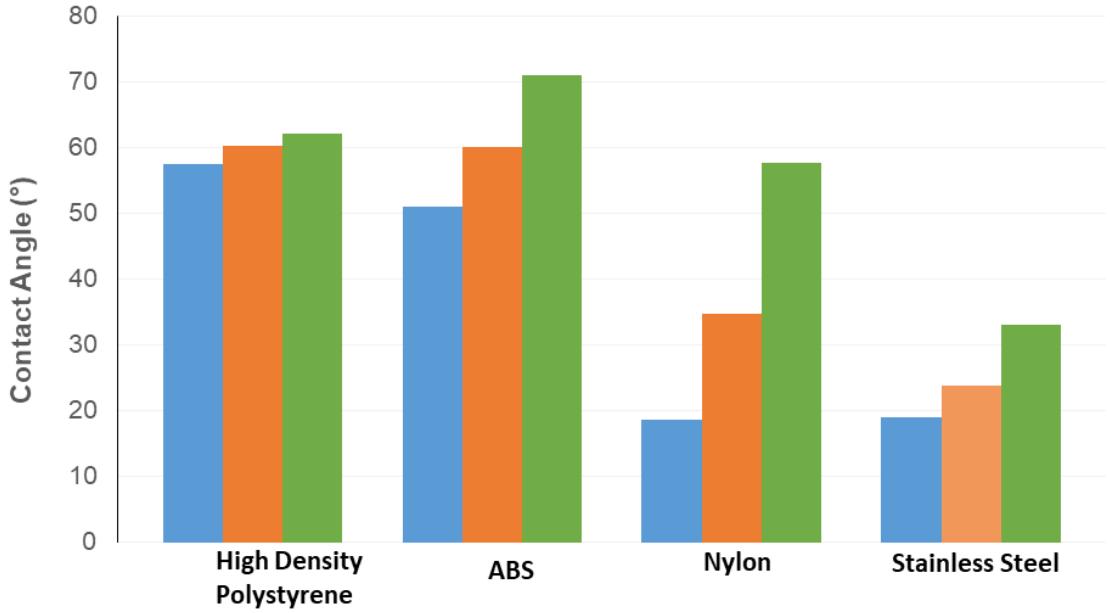

Figure 20. Contact angle of aqueous amines (at different carbon loadings) on different packing material surfaces.

LLNL worked in parallel on post-processing surface treatments that can increase and/or decrease the contact angle of these polymers. A post-printing hydrophobic spray coating was applied and yielded a > 50% increase in the contact angle; however, the coating was not stable to high temperature amine exposure. After ~2000 hours at 60 °C the coating was visibly removed, and the contact angle measure the same as the underlying polymer. Better results in decreasing the contact angle of the polymers were obtained using a post-printing (<10 sec) acetone dip/drying. **Figure 21** shows the contact angle of water against the HDPS after the acetone dip measured over a few weeks period. The contact angle decreased after the acetone dip. After 16 days the polymer was thoroughly washed with water, and the contact angle returned to its original value suggesting that this post-processing technique is not a viable option to increase hydrophobicity.

Beyond surface modifications, the surface tension and contact angle (vs. polymer surface) of the amine solvents can be modified by adding a surfactant additive. In one example, the contact angles of a reference amine solvent with a small amount of surfactant (0.01 wt.%) at different carbon loadings was measured on all the packing material surfaces (**Figure 22**). The addition of surfactant lowers the contact angle of the solution versus the HDPS, Nylon and ABS surfaces. The contact angle changes on SS with were within the uncertainty of the experiment. This shows that the wettability of the aqueous amine solvent on these polymeric packing materials can be enhanced by adding a surfactant like.

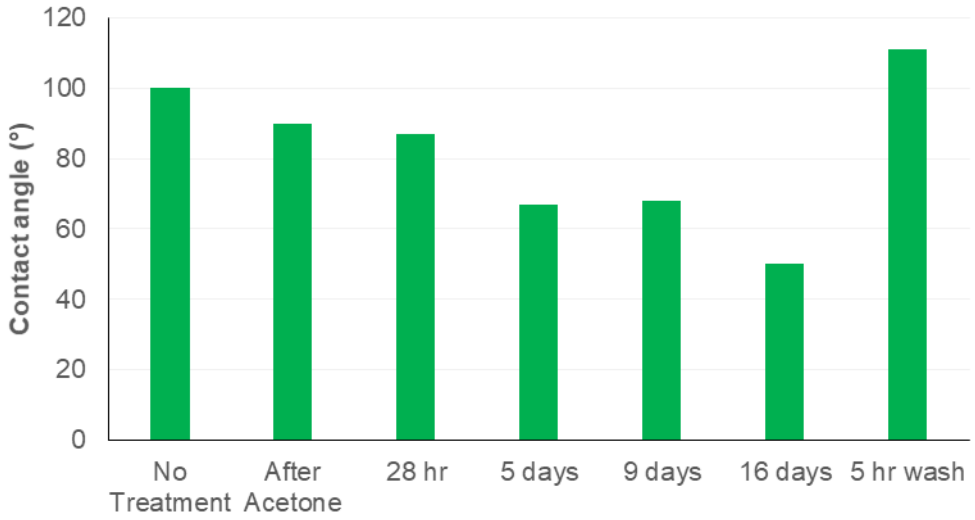

Figure 21. Contact angle of water versus a HDPS surface after a post-printing acetone dip treatment.

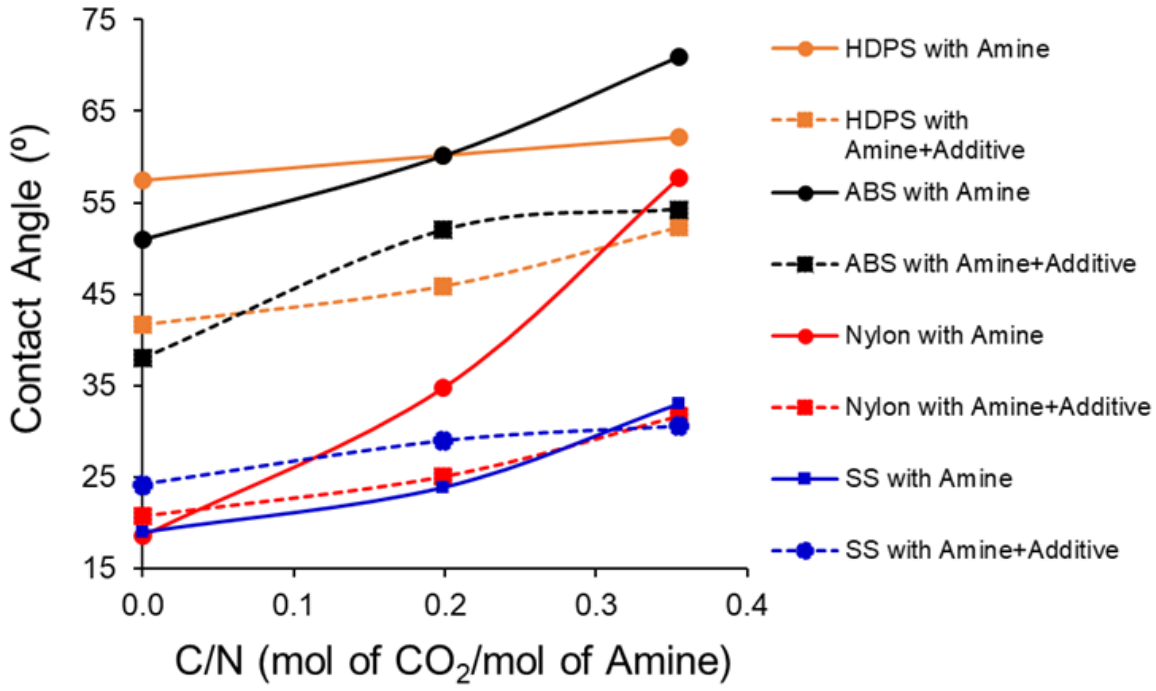

Figure 22. Contact angle of amine solvent with an additive at variable CO_2-loading on different packing materials surfaces.

3.2.2 Development and Fabrication of Custom Packing

The durability of the candidate polymeric packing materials regarding hydrophobicity in the corrosive amine solvent environment was evaluated. Polymer coupons were prepared by LLNL for use in amine stability testing; Nylon, HDPS, ABS, and Poly-lactic acid (PLA). The contact angle of each material (after polishing) was measured with water, and a CO_2-rich amine solvent solution prior to exposure to the amine solution (**Figure 23**). The weight and diameter of each coupon was also measured prior to amine exposure. The polymer coupons were placed in the amine solvent for 1000 hrs. at room temperature, after which they were removed, and the measurements were repeated. The coupons were then returned to the amine solvent for an additional 1000 hrs. at 60 °C. The coupons were again removed and the weight, diameter and contact angle measurements were repeated. To date the coupons have been exposed to the CO_2-rich amine solvent for 6000 total hours (1000 h at room temperature + 5000 h at 60 °C) (**Figure 24**).

Figure 23. Polymer coupon before (top) and after exposure to CO_2-rich amine solvent solution 6000 total hours (1000 h at room temperature + 5000 h at 60 °C except PLA which only after 1000 h at room temperature).

The HDPS, ABS and Nylon polymers were essentially unchanged in term of contact angle (vs water and amine solution) after 4000 total hours (1000 h at room temperature + 3000 h at 60 °C) exposure to the CO_2-loaded amine solvent. Both versions of PLA decomposed after being exposed to the amine solvent at elevated temperatures. Due to the good stability, HDPS, ABS and/or Nylon will be further evaluated as material candidates for the hydrophilic/hydrophobic segments.

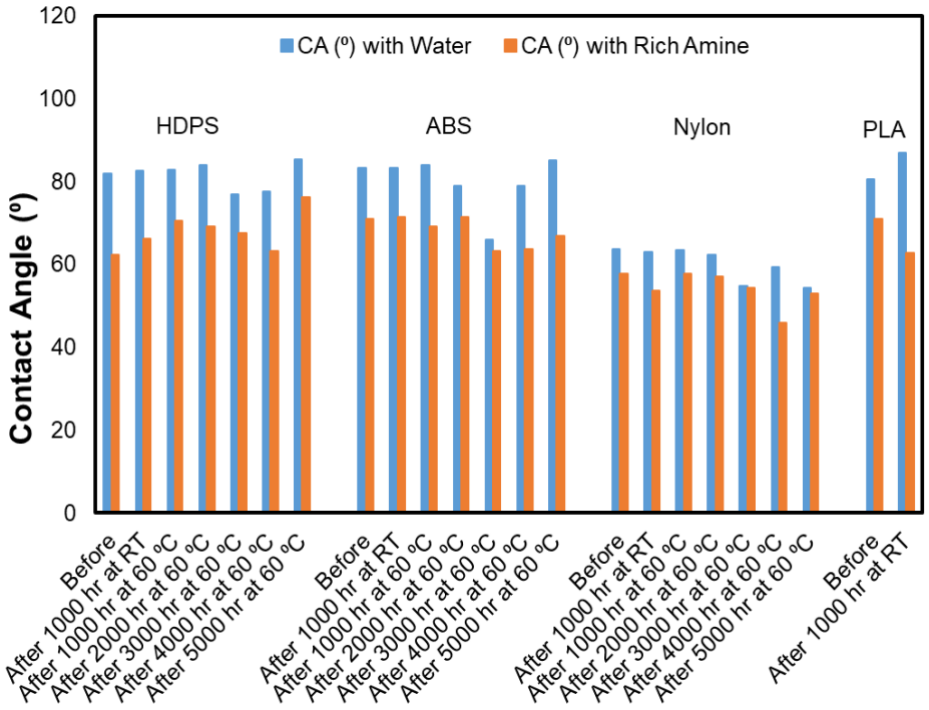

Figure 24. Contact angle (°) changes of polymeric materials after long-term exposure to CO_2-loaded amine solvent.

LLNL conducted some CFD modeling activities using OpenFoam software to better understand the liquid distribution through the packing surfaces. **Figure 25** shows the modeling from surfaces with contact angles at 0° (blue), 50° (yellow) and 90° (red) along with alternating 50° + 90° (green) surface, like the co-printed dynamic packing. Below this is the corresponding calculated wetted surface areas for these same packing surfaces with different contact angles. The best surface coating and corresponding highest wetted surface area is the 0° contact angle, essentially a purely hydrophilic surface. Interestingly, the next best surface is the alternating 50° + 90° (green) surface where the movement caused by the alternating relatively high and low hydrophobic surfaces has increase the overall wetted surface area and liquid distribution. This behavior should lead to an increase in solution mixing and mass transfer when applied in a CO_2 absorber column.

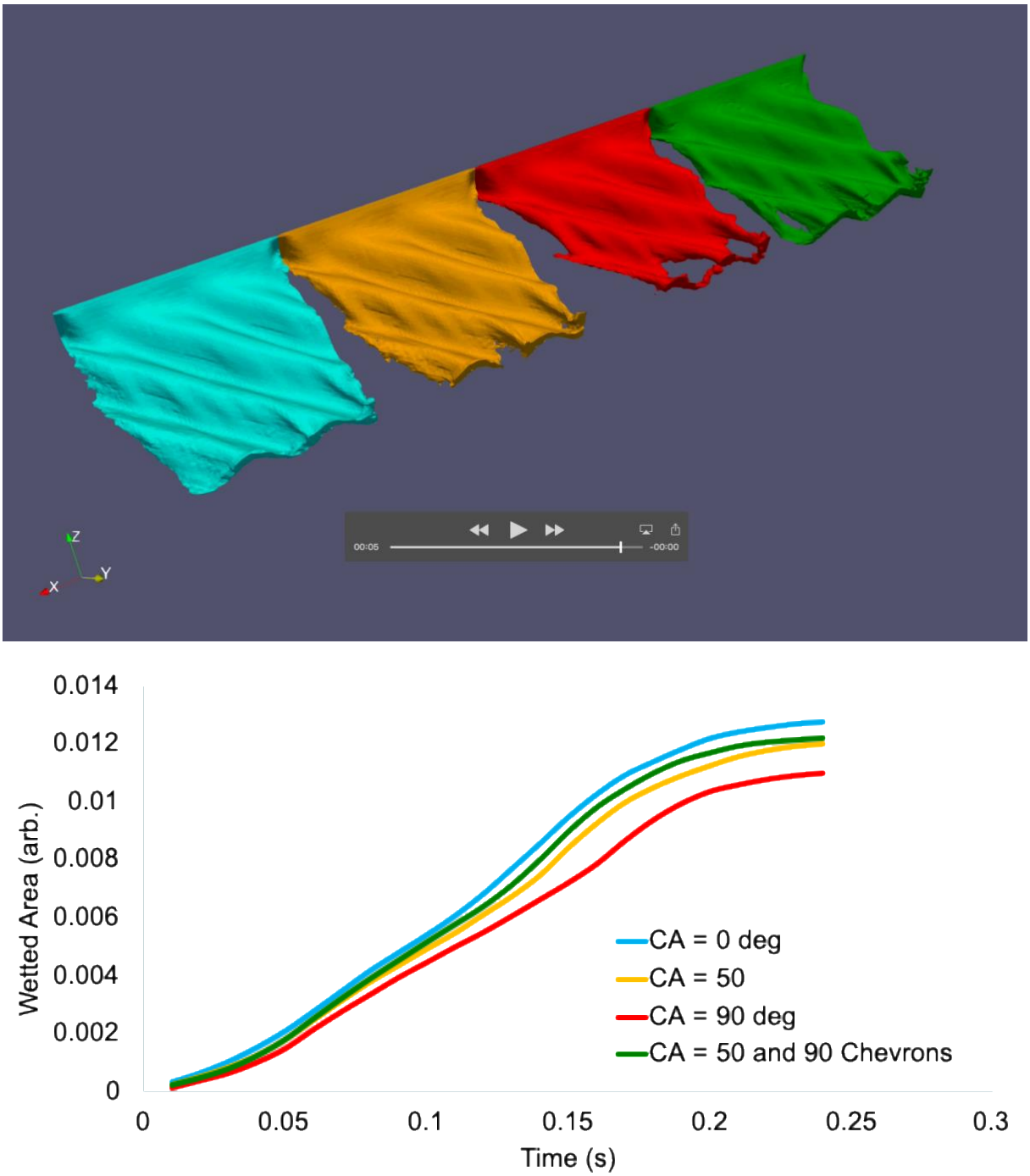

Figure 25. Liquid distribution modeling of surfaces with different contact angles (CA) as a measure of relative hydrophobicity with the amine solvent.

Using the polymer candidates identified previously, LLNL developed several dynamic packing (co-printed) patterns (**Figure 26**). During the testing printing, it was observed that there was an adhesion problem between the Nylon and ABS polymers, with some of the overlaid white ABS patches falling off easily. Two causes were identified, first the 3D printers at LLNL were being

heavily used and the print heads were not being adequately cleaned between prints. There was also contamination of the printer head with different polymers during this time. These issues were addressed, and the next set of test prints has noticeably better adhesion.

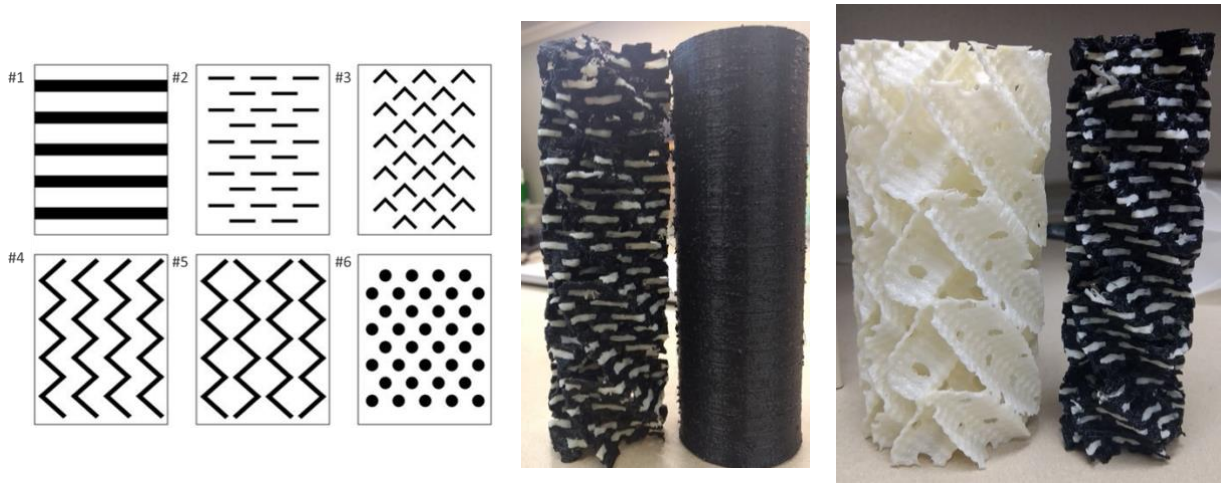

Figure 26. Initial pattern designs of co-printed (dynamic) polymer packings (left); test print of pattern #2 with Nylon (black) as the base and ABS (white) as more hydrophobic sections with both an open and closed configuration (middle); ABS 250Y 3D printed packing and 250Y dynamic packing (right).

3.2.3 Fabrication of Custom Packing

The original plan was for LLNL to identify commercial fabricator(s) capable of producing the optimized dynamic packing material to the specification defined by LLNL and UK. However, based on the size and complexities of the dynamic packing, LLNL was able to handle the printing duties internally and print enough packing for the entire absorber column (**Figure 27**) that was used during the long-term testing (Task 8)

Figure 27. Dynamic packing produced by LLNL and used during long-term testing (Task 8)

3.3 Testing Plan Development (Task 4)

An appropriate parametric test matrix was developed to evaluate the dynamic packing and solvent. In this task, Design of Experiments was used to reduce experimental load, while obtaining good prediction and representation. A one-third fractional design was adopted with three levels for each variable, which contained up to three independent variables to evaluate the solvent and dynamic packing performance. The three variables were: liquid recirculation rate, stripper pressure, lean solvent temperature. The main system performance targets were (1) CO_2 capture efficiency, and (2) energy consumption. The baseline steel and each different version of the dynamic packing were tested at each parametric condition and the stable CO_2 capture efficiency and energy consumption were calculated for each condition.

There is a certain amount of variation in the integrated unit regarding various fluid flow. To better understand the possible mechanism of parameter effects, a parametric study is required to reduce the sensitivity for the integrated system. The CO_2 concentration, temperature and flow rate of inlet mixed gas will be fixed without any changes. Based on our previous work, we screened four system variables, i.e., hot oil circulation rate, lean return solution temperature, amine solution circulation rate and stripper pressure, to give a comprehensive evaluation. The parameters will be tested at three levels as tabulated in Table 1 to quantify the parameter sensitivity. We are also interested in the impact of surfactant, so the additive concentration is listed as an influential parameter in the **Table 1** as well. A detailed discussion of each primary variable is included below.

Table 1. Initial parametric study of integrated bench unit

Variable and Condition	Level 1	Level 2	Level 3
Hot oil circulation rate, L/min	5	10	15
Amine solution circulation rate, mL/min	300	500	700
Lean return solution temperature, ˚C	30	40	50
Stripper pressure, kPa	120	150	180

Hot Oil Circulation: CO_2 stripping and amine solution regeneration consumes most energy in the entire carbon capture process. In the integrated bench unit, hot oil circulation is responsible to provide adequate energy to the stripper. Controlling the circulation of hot oil means management of reboiler duty (Q) and energy input to the amine solution regeneration. The hot oil flow in the stripper bottom sump jacket is adjusted through a bypass where a certain amount oil stream return to circulator straightly. This will change the effective oil flow rate and internal heat transfer heat in the jacket. It is expected that increase the oil flow rate should lead to higher heat duty and amine solution regeneration temperature in the stripper. CO_2 loading of lean return solution could be lower to allow a higher CO_2 absorption efficiency in the absorption column. However, the energy demand for capturing per mole CO_2 may increase due to greater reboiler duty and energy consumption.

Amine Solution Circulation Rate: The amine solution circulation rate can be adjusted via the needle valve set in the lean return solution line. As described before, rich solution stream shares the same flow rate as that of lean return solution. Hence the lean return solution flow rate is equal

to amine solution circulation rate. Adjustment of amine solution circulation rate will change liquid gas ratio (L/G) sine gas flow rate is fixed in this investigation. Increase amine solution flow rate means higher liquid gas ratio. This will increase the wettability of packings in the absorption column to provide larger contact area for mass transfer between liquid and gas phase. As a result, the CO_2 absorption efficiency and working capacity of the integrated bench unit will be improved. However, there is an upper limitation to the working capability, which is dependent to the column size like inner diameter. Furthermore, the increase of amine solution circulation rate should drop the amine solution temperature in stripper with some unfavorable influences. The poor amine solution regeneration performance will result in lower lean return solution CO_2 loading. Lower regeneration amine solution temperature can cause higher heat duty and energy consumption. And the increase of amine solution circulation rate requires more work from rich and lean pumps.

Lean/Rich Temperature: The lean return solution temperature at the inlet of absorption column determines the CO_2 absorption temperature along with whole column. After being heated to higher than 100 ˚C for regeneration, the lean return solution is sent to heat exchange to recycle a portion of heat energy. Then the lean return solution temperature is precisely tuned through a bypass polisher before entering the absorption column. The inlet temperature covers 30, 40 and 50 ˚C as the typical lean return solution temperature. Higher solution temperature should be beneficial for CO_2 molecule diffusion from liquid gas interface into bulk solution. And the chemical reaction between amine and CO_2 will be faster from kinetic perspective. Higher CO_2 absorption temperature could improve the efficiency. However, considering the CO_2 absorption as an exothermic process, the increase of temperature will decrease the maximum CO_2 loading and reduce the driving force between operation line and equilibrium line. The excessive temperature increase could be disadvantageous for CO_2 absorption. In the top section of absorption column, the CO_2 loading of amine solution is low and carbamate formation dominates the CO_2 absorption process. This process is kinetically driven since carbamate formation is a fast reaction. But in the bottom section of column, the amine solution reaches high CO_2 loading region and CO_2 absorption driven force shifts to (bi)carbonate formation and physical absorption, which can be considered as thermodynamic control. Consequently, there could be an optimum inlet temperature to achieve lowest outlet CO_2 concentration and highest overall absorption efficiency.

Stripper Temperature: In stripper site of the integrated bench unit, the pressure is always higher than absorption site due to the higher temperature. The rise of temperature will cause CO_2 release and water evaporation, elevating stripper pressure accordingly. On the other hand, increasing pressure can also lead to the rise of amine solution temperature. And it is noted that higher amine regeneration temperature is beneficial to reduce heat duty with fixed hot oil flow rate. Therefore, a back-pressure regulator is mounted in the outlet line of stripper to control and further increase stripper pressure without additional energy input. Ideally, the pressure builds up will result in a higher amine solution temperature in stripper to reduce heat duty. But the pressure builds up attributed to higher CO_2 partial pressure is disadvantageous to amine regeneration because of thermodynamic limitation. In another word, using released CO_2 to build up pressure and increase amine solution temperature lacks driving force for further CO_2 stripping. Therefore, the lean return solution will have higher CO_2 loading and CO_2 absorption efficiency will be reduced.

3.4 Bench-scale Testing of Dynamic Packing Material (Task 5)

The primary controllable variables on the UK small bench CO_2 capture unit are the liquid and gas flow rates, inlet gas CO_2 concentration and temperature, lean amine temperature, and stripper operating temperature and pressure. The solvent testing showed that the data collected from the small bench CO_2 capture system was consistent from day-to-day with variability of ± 5% on average. First, baseline testing was conducted with stainless steel Mellapak 250Y 3" packing with the UK solvent. Next, testing of sections of 3D printed 250Y from ABS was conducted. The energy consumption and capture efficiency with the 250Y steel and ABS packing was generally similar and within the measurement errors and reproducibility of the unit. During the printed ABS testing it was observed that the solvent was channeling to the column walls to a greater extend compared to the steel packing. An in-situ liquid re-distributor will be installed below the printed ABS packing to minimize the channeling. Next, three different patterns of dynamic packing were installed in the upper portion of the absorber column.

3.4.1 Baseline Solvent Testing

The UK solvent was used in the baseline testing with 72 inches of conventional 250Y steel structured packing in the absorber column. Several baseline testing runs were conducted to develop a set of general operating parameters and collect baseline data to be used as a comparison against the performance when the 3D printed dynamic packing is installed.

Table 2 gives a summary of the initial data collected from the UK solvent and the conventional SS 250Y packing installed in the absorber column. The CO_2 capture percentage and energy demand are in the general ballpark of previous solvent testing performed on this unit with its 3" absorber column. The lean and rich CO_2-loading of the solvent have room for improvement through implementation of the dynamic packing and enhanced solvent.

Table 2. UK solvent performance/data collected from the UK small pilot integrated CO_2 capture unit with 250Y stainless steel packing.

Inlet Conc.CO_2%	14.26%	14.18%	14.12%	14.17%	14.31%	14.44%
Q, Reboiler, KW	1.40	1.39	1.35	1.33	1.35	1.32
Stripper Pressure, kPa	120.65	120.66	118.46	118.85	118.07	118.80
Reboiler bulk solvent TC	107.09	106.97	106.61	106.47	106.38	106.66
Total Alkalinity, mol Alk./kg	4.28	4.06	4.86	4.81	4.75	5.13
Carbon Loading, mol CO_2/kg	1.84	1.97	2.11	1.96	2.03	2.17
C/N, mol CO_2/mol Alk. (Rich)	0.43	0.49	0.43	0.41	0.43	0.42
C/N, mol CO_2/mol Alk. (Lean)	0.26	0.27	0.30	0.29	0.27	0.28
CO_2 absorption efficiency	62.0%	61.6%	60.2%	59.0%	57.8%	59.2%
Energy Demand (kJ/mol CO_2 captured)	176.36	178.76	178.68	179.41	184.91	173.55

3.4.2 Installation of Dynamic Packing into UK Bench CO_2 Capture Unit

The steel 250Y structured packing material inside the absorber column in the bench-scale CO_2 capture unit was first replaced with section of 3D printed ABS packing (**Figure 29**), then replaced by the dynamic packing (**Figure 30**) at only the top 18" of the absorber packing due to limitations in packing production capacity. For most advanced solvents the temperature bulge occurs at the top of the absorber packing therefore it should be easy to see enhancements by only replacing the

packing in this top section. Minor absorber modifications were needed to accommodate the polymeric packing material. A new differential pressure gauge was installed to accurately monitor the pressure drop across the absorber packing. A pressure regulator was also installed on the CO_2 product stream exiting the stripper to better control the stripper pressure and solvent regeneration temperature.

Figure 28. Stainless steel Mellapak 250Y packing material with 3" diameter.

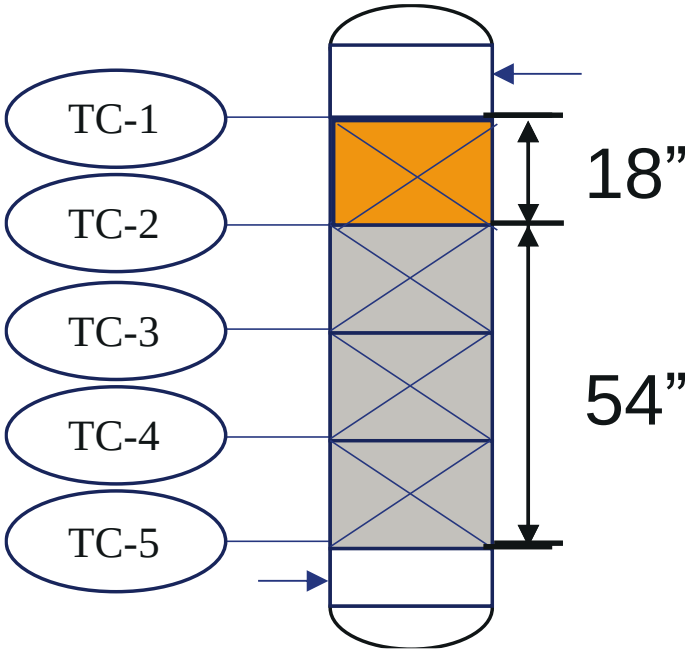

Figure 29. Column configuration with replacement of 18" of the packing on top of 54" of stainless steel Mellapak 250Y packing material with 3" diameter.

3.4.3 Bench-Scale Testing of Dynamic Packing for Mass Transfer Enhancement

Based on the CFD modeling and printing limitations three DP packing designs were produced and compared to the baseline steel packing. The three designs are shown in **Figure 30**. The DP packings have the same geometric general structure as the steel packing with an additional HIPS shell. The internal packing surface is printed according to the different patterns as shown in the bottom right corner of each figure. DP-1 and DP-3 packings have 5% (of total surface) of HIPS embedded in the nylon packing surface with smooth transition flat plane between two materials, where the HIPS segment is in the form of a staggered rectangle strip for DP-1 and a "V" shape for DP-3. DP-2 packings have alternative full 12.7-mm segments with HIPS (50% of total surface) and nylon (50% of total surface). The solvent from the hydrophilic segment will either pass over a hydrophobic packing surface or be repelled by the hydrophobic shell before entering the next hydrophilic segment, which is expected to sufficiently improve the liquid spread and mixing effect within the absorbent. In the preliminary experiments, it was found that the temperature bulge existed at the upper part of the absorber column under given conditions, indicating that most of the CO_2 is captured in this section. Therefore, each type of DP packing was printed in total 457.2 mm and installed in the upper part of the absorber column during the tests.

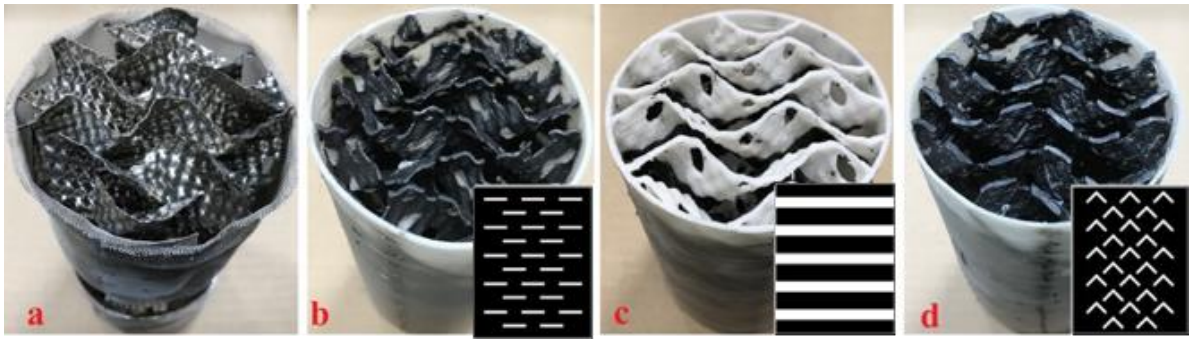

Figure 30. Mellapak 250Y steel packing (a); DP-1 packing (b); DP-2 packing (c); DP-3 packing (d).

A parametric study was carried out for each packing installed to optimize operating conditions. The CO_2 capture results for all cases were summarized in **Figure 31** in terms of absorption efficiency and the energy demand at corresponding run. The bubble size indicates the relative heat duty at corresponding condition. In general, when comparing with steel packings, the application of DP packings enables the cases to be shifted toward the further bottom right which means an improved system performance. The cases using DP-3 packing exhibit the best performance of high CO_2 absorption efficiency and low energy demand. Changing the L/G ratio could affect liquid holdup in the column while absorbent residence time could vary in the reboiler due to the constant system liquid inventory. Increasing stripper pressure requires high solvent regeneration temperature and impacts the gaseous CO_2/ H_2O ratio at stripper top. These would cooperatively impact CO_2 loading in the lean/rich absorbent and working performance of the absorber/stripper.

Overall, operating under 2.6 L/G ratio and medium to high stripper pressure is optimal for the current unit regarding both CO_2 absorption efficiency and energy demand. Such influences are similar for those cases using different packings. In the experiments with fixed packing height, the improvement in mass transfer with DP packings may not be revealed if the packing height is overdesigned. All three DP packings have better performance than steel packing under given conditions. Using Mellapak 250Y steel packing as the baseline, there is a relative 7.8%, 7.7%, and 9.1% improvement in CO_2 absorption efficiency and consequential 7.0%, 7.9%, and 8.4% energy penalty reduction for DP-1, DP-2, and DP-3 packings, respectively. Higher heat duty improves CO_2 absorption efficiency by returning leaner solvent to the absorber which could be interpreted the mass transfer is dominantly controlled by reaction kinetic and the diffusion resistance is minimized with application of DP Packings.

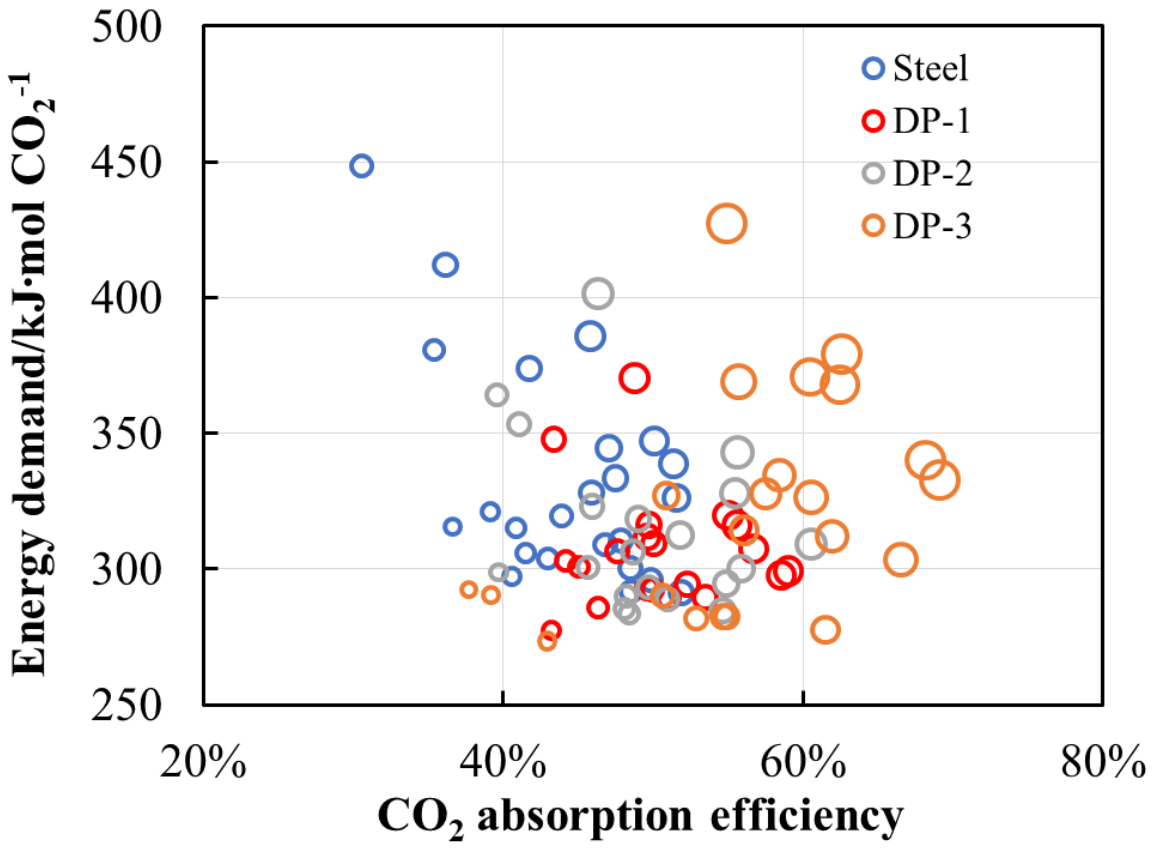

Figure 31. Energy demand versus CO2 absorption efficiency for all cases through parametric study, where bubble width indicates the heat duty.

3.5 Bench-scale Testing of Additive Modified Solvent (Task 6)

UK solvent, and additive enhanced UK solvent will be evaluated against conventional Mellapak 250Y stainless steel packing installed in the absorber of the UK small bench CO_2 capture unit.

3.5.1 Additives Selection and Procurement

Using the findings from Task 2 and 3, the UK solvent and additive were obtained in sufficient quantities for testing on the UK small bench CO_2 capture unit.

3.5.2 Bench-Scale Testing of Additives for Mass Transfer Enhancement

The UK solvent was enhanced with surfactant-like additive which reduced the surface tension from above 60 to below 50 mN/m. This brings the contact angle on the steel surface to a similar level as that on the nylon surface (**Figure 32**). This translates to no significant difference in wettability for those two materials when the additive is is used for CO_2 absorption. The contact angle data highlight the benefit of using surfactant-like additive to decrease the solvent surface tension when polymeric packings are used for absorber construction and cost reduction. It also needs to be mentioned that the additive can either increase or decrease mass transfer at gas–liquid interface

depending on its concentration. In this study the concentration of the additive was selected based on lab-scale screening during which mass transfer was enhanced. For the DP packings containing nylon and HIPS, the contact angle shows around 13–18° difference on those two materials to serve as driving force for enhancing turbulence.

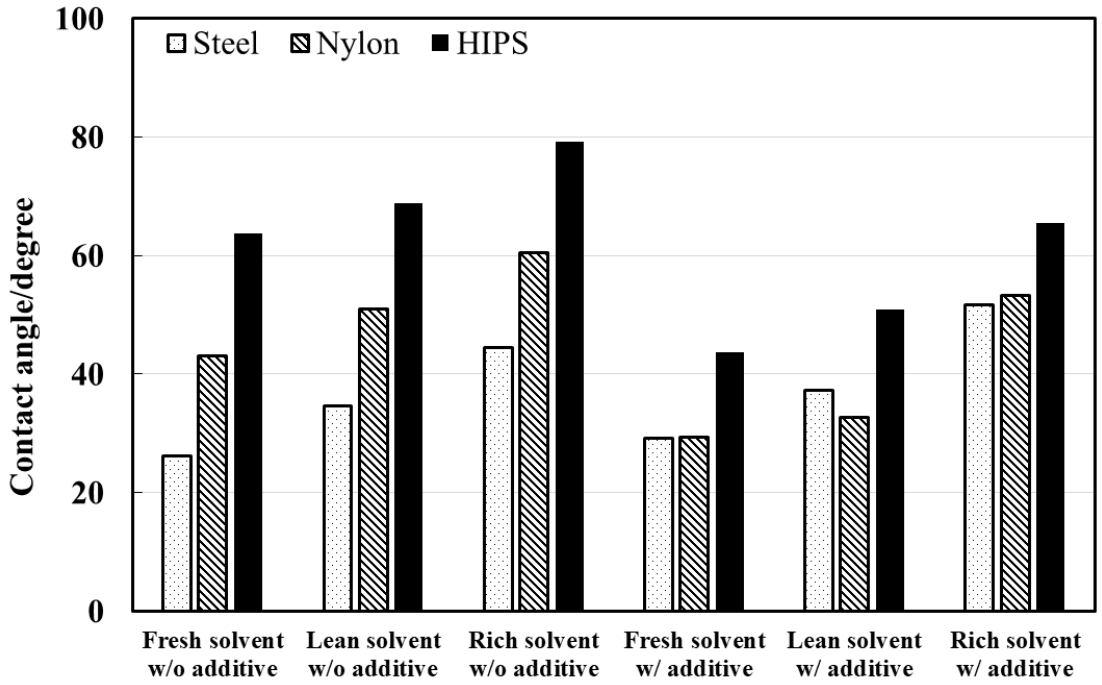

Figure 32. Contact angle of an amine solvent different surfaces with and without a surfactant additive. The CO_2 loading of fresh, lean, and rich solvent are 0, 0.247, and 0.471 mol CO_2/mol amine.

3.6 Testing of Electrochemical Cell for Nitrosamine Decomposition (Task 7)

The goal of this task was to develop a process to neutralize nitrosamines derived from amine solvents using an electrochemical treatment. Nitrosamines (as a class of compounds) can be decomposed through an electron transfer to re-form a secondary amine. To further develop this approach, initially a small electrochemical cell was prepared using a UK-developed carbon electrode material. The characterization of the electrode material was performed, followed by nitrosamine decomposition testing to determine the mechanism of decomposition, and calculated the efficiency of the process. General operating parameters of the electrochemical cell were identified. Application of the developed process to simulated waterwash solutions containing nitrosamines initially showed a greater than 60% reduction in nitrosamines with an efficiency above 10%, surpassing the milestone for both metrics. Finally, the electrochemical cell was scaled-up and tested in a flow-through process to further increase decomposition rates (> 90%) while increasing efficiency (> 15%).

3.6.1 Electrode Material Synthesis and Operating Condition Selections

The UK-developed carbon electrode material, known as carbon xerogel (CX) is synthesized from a carbon cloth pyrolyzed with a resorcinol-formaldehyde gel creating a conductive, high surface area mesoporous (20 Å – 500 Å or 2nm – 50nm) material. Nitrosamines can be adsorbed directly onto the carbon CX material under neutral and basic conditions with a relative high capacity (10-40 mg/g). This adsorption component can be advantageous as the CX electrodes can be used to first separate the nitrosamines from the dilute wastewater stream, such as the amine CCS waterwash, followed by electrolysis of the adsorbed compounds intermittently, rather than in a continuous operation mode. Further cell development was conducted through running a cyclic voltammogram (CV), in a half-cell configuration, of the CX electrode in the presence of nitrosamines (surrogate nitrosamines nitrosodiethylamine (NDEA) and nitrosopyrrolidine (NPY) were used in all experiments). The CV showed peaks at both positive and negative voltage scan. This indicated that nitrosamines can be oxidized at anode and reduced at cathode when charge is passed through the cell. In this configuration the CX electrode material can be used as both the anode and cathode in the combined electrochemical cell.

Two small cells were constructed to perform additional mechanistic and operation testing. E-cell NACX0 (**Figure 33a**) is a typical batch-style of two electrode cell with the CX as the anode. **Figure 33b** shows e-cell NACX1 designed to reduce the distance between anode and cathode using a sandwich structure with CX as both the anode and cathode with a shortened distance between the electrodes resulting in an increase in the efficiency of the electron transfer.

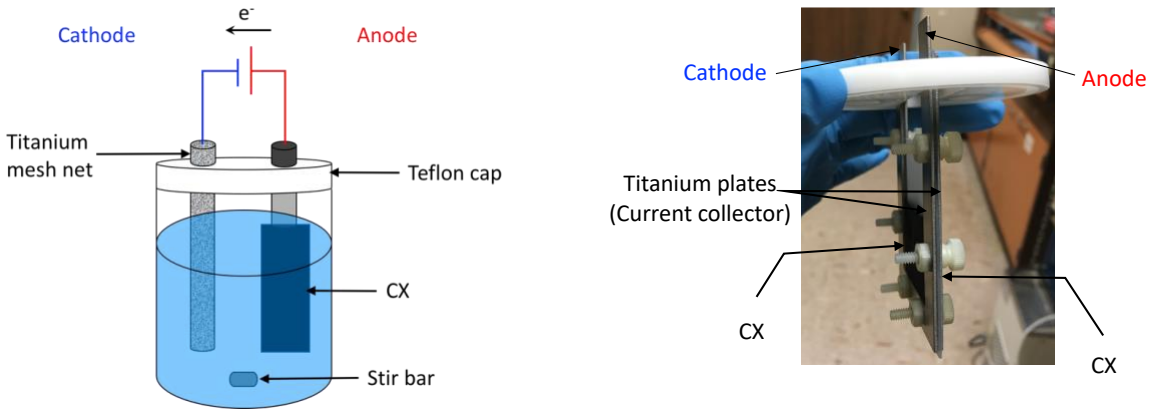

Figure 4.7.1. Scheme of electrochemical cells for nitrosamine decomposition using (a) NACX0, and (b) NACX1.

The electrolysis of nitrosamines from a simulated waterwash solution, which included 1 wt.% MEA, was plotted against applied constant charge at 5-300 mA for 1 hour using e-cell NACX0 (**Figure 34)**. The calculated total charge efficiency of the decomposition reaction was also calculated and included in this plot. The removal of nitrosamines increased as the total charge passed increased, along with a corresponding increase in cell voltage. At currents above 50 mA the cell voltage exceeded 6 V, leading to visible anode degradation. At a current of 25 mA, the anode showed no visible signs of degradation, while the nitrosamine decomposition was close to the target removal percentage.

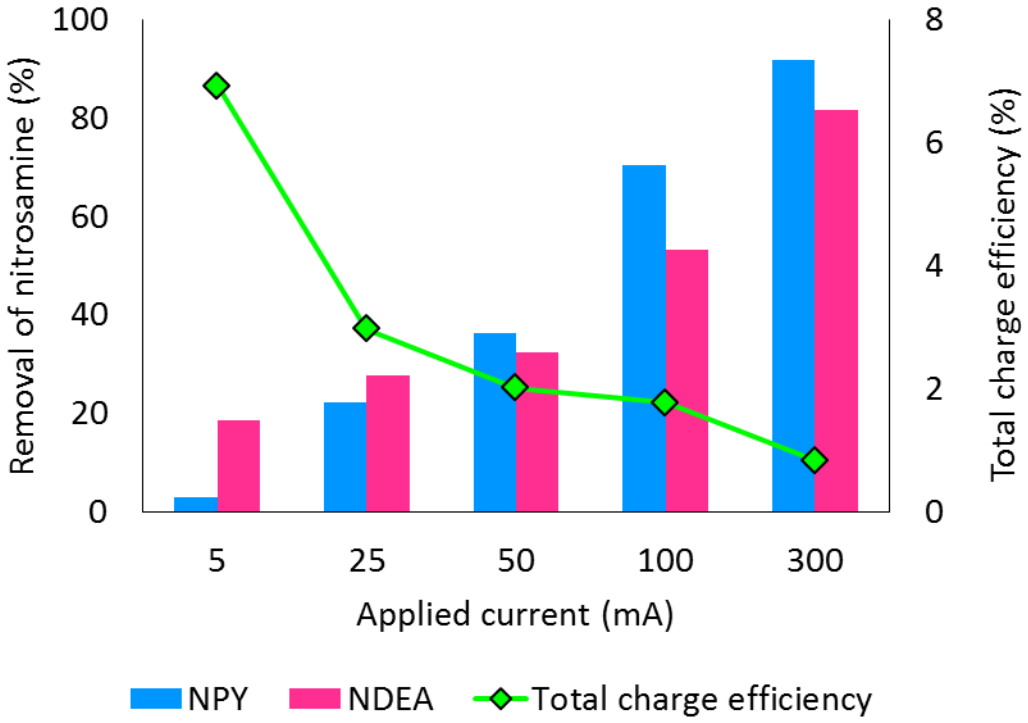

Figure 34. Removal of nitrosamines from solution with different applied current for 1 hour (in 1 wt.% MEA simulated waterwash solution) using NACX0 cell. Total charge efficiency was calculated.

Next, electrolysis using NACX1 cell at 25 mA and 100 mA in a simulated waterwash is plotted as a function of time for adsorption (**Figure 35**). These two processes, adsorption and then electrolysis at 100 mA and 25 mA achieved more than 60 % removal of nitrosamines from simulated waterwash using NACX1 cell. Although the higher charge at 100 mA enabled to remove nitrosamines from waterwash faster than lower charge at 25 mA, total charge efficiency at 100 mA was lower than at 25 mA. Total charge efficiency of electrolysis at 25 mA achieved >10 %, while the efficiency of electrolysis at 100 mA could not. Using the 25 mA charge value, the milestone targets of 60% removal with an efficiency of 10% was achieved.

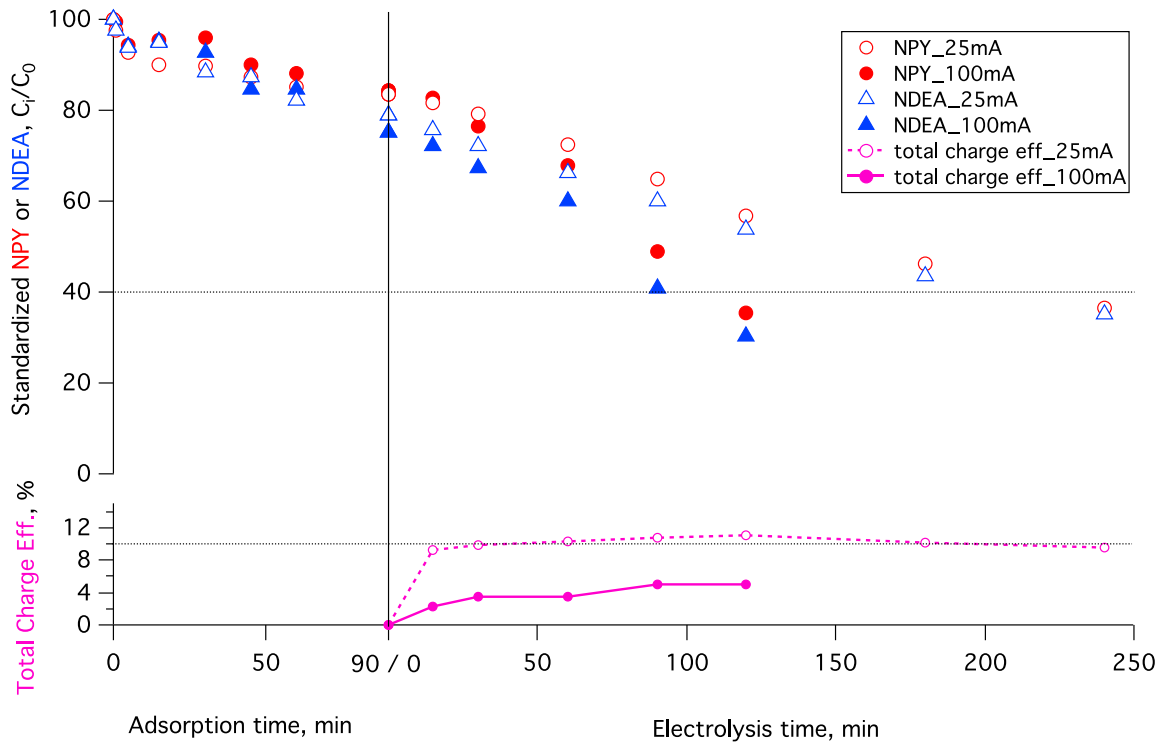

Figure 35. The removal of nitrosamine from a simulated waterwash by adsorption and electrolysis as a function of time. Electrolysis was performed at 25 mA and 100 mA. The total charge efficiency is calculated for both charge values (dashed lines indicate milestone targets of 60% removal and charge efficiency of 10%).

After selecting the optimal operating charge value of 25 mA a flow through electrochemical cell was designed and fabricated (**Figure 36**). Operating parameters of the flow through electrochemical cell were further optimized at difference liquid flow rates and at different nitrosamine concentrations. The removal behavior of nitrosamines four flow rates through the e-cell flow are shown in **Figure 37**. The nitrosamine concentrations in each figure have been standardized to for easier comparison between the four flow rates. The flow rate of the flow through e-cell system impacted the removal efficiency of both nitrosamines from the solution during the 16-hour electrolysis period, with higher flow rates leading to slower removal behavior. A flow rate of 40 mL/min presented the slower removal efficiency than the other flow rates, removing only ~ 65% total nitrosamines after 16 electrolysis operating hours. Both lower flow rates, 20 mL/min and 10 mL/min, reached removal efficiencies < 98% after 16 hours of operation, presenting the most efficient removal behaviors in this e-cell. This trend is likely due to the residence time of the solution within the e-cell.

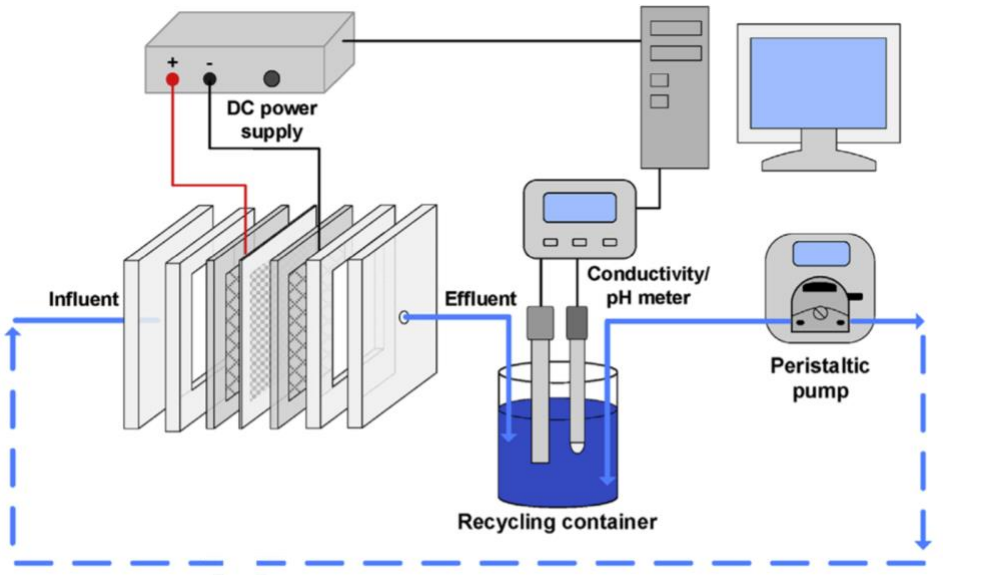

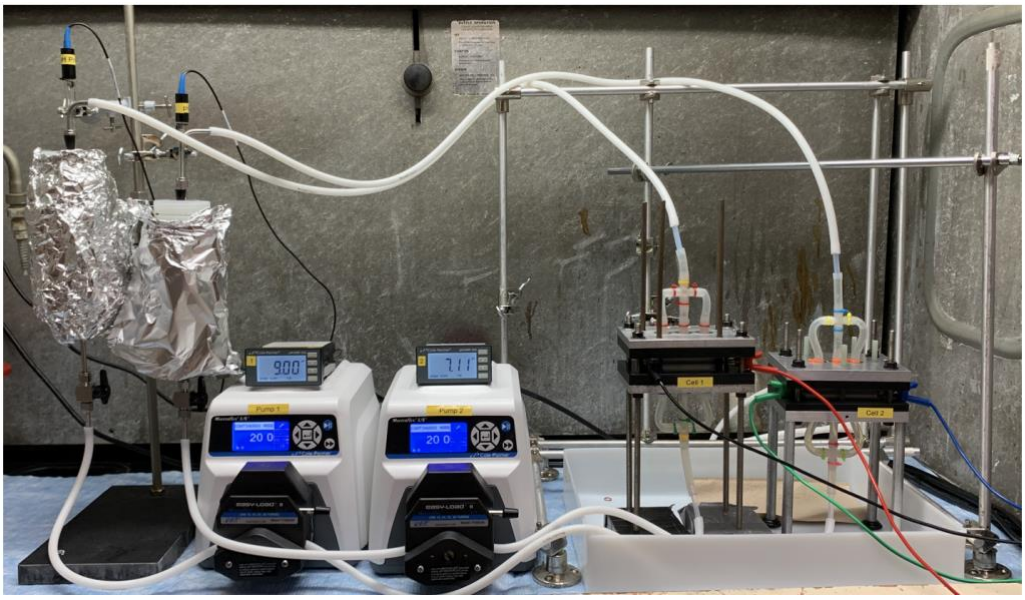

Figure 36. Flow through electrochemical cell for decomposing nitrosamines.

Although the faster flow rates have faster solution turnover rates, they lead to shorter residence times in the e-cell chamber, which are most likely too quick for ideal contact with the electrodes where the reduction occurs, leading to lower removal efficiencies. The flow rates of 10 and 20 mL/min both have similar removal efficiencies but have different residence times and solution turnover rates. Although at 10 mL/min the residence time is longer the solution turnover time is greater and given similar nitrosamine removal performance to a 20 mL/min these results suggest that the ideal flow rates for this e-cell operation is 20 mL/min.

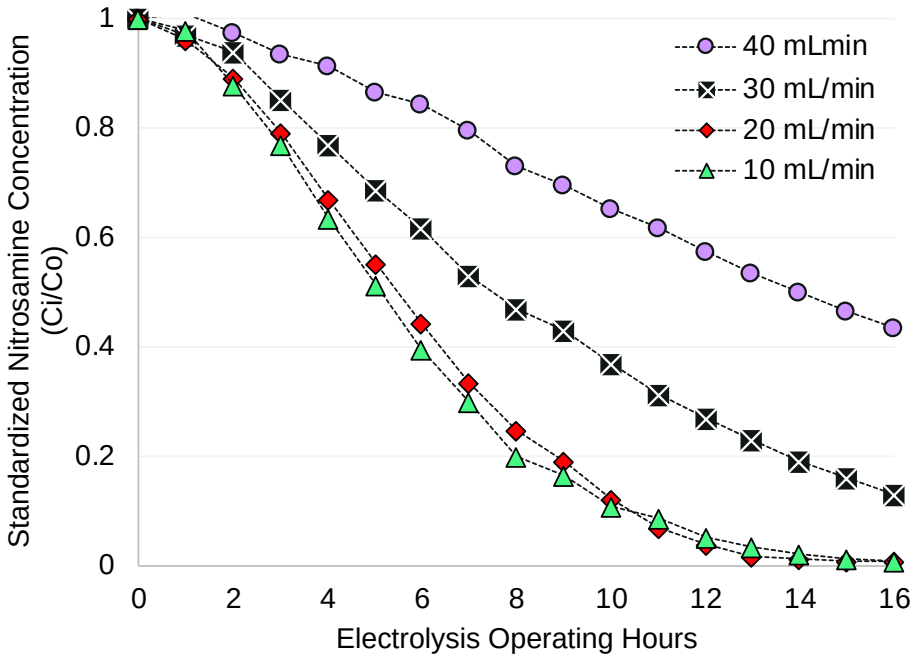

Figure 37. The nitrosamine removal behavior at four flow rates using a flow-through e-cell with simulated waterwash as a function of time.

Using this ideal flow rate impact of nitrosamine concentration on e-cell performance was investigated. Around 30, 100, 200 and 400 ppm nitrosamines were spiked into solution for each experiment, the results are presented in **Figure 38**. At lower concentrations, our limit of detection (LOD) was reached within 8 hours of operation shown in pink. At 100 ppm nitrosamines LOD was reached within 10 hours of operation and at 200 ppm LOD was reached in about 14 hours of operation, in green and red respectively. When the concentration of nitrosamines in the cell exceeds 200 ppm the removal rates were impacted significantly, with only about 60% of the nitrosamines decomposed in the solution over the 16-hour electrolysis period. Based on this data, the cell in its current configuration is at its most efficient with regards to removal rate at concentrations less than or equal to 200 ppm.

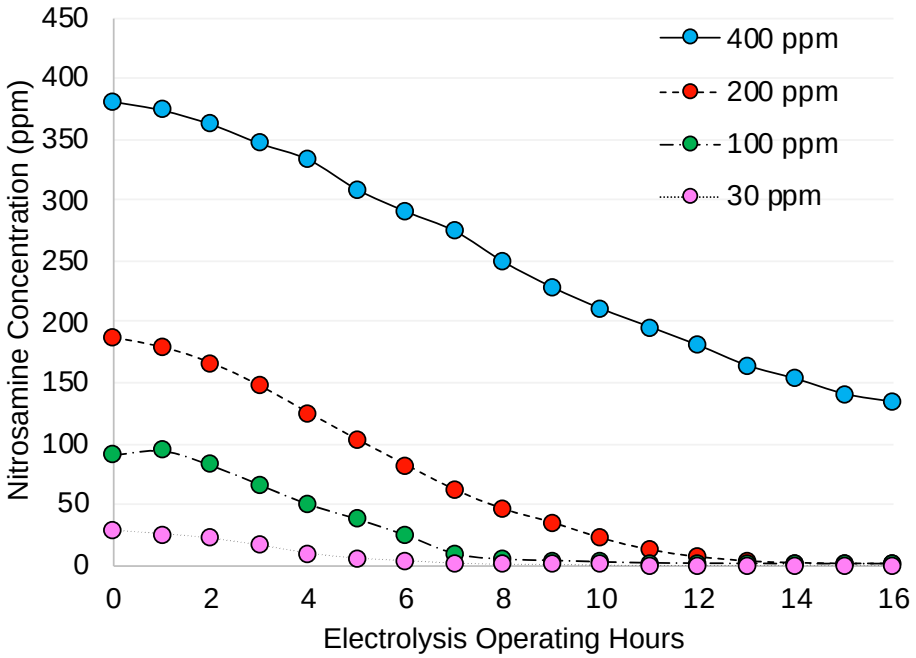

Figure 38. The nitrosamine removal behavior at different initial concentrations using a flow-through e-cell with simulated waterwash as a function of time.

Using this knowledge, the performance of the e-cell was investigated under these optimized conditions, a flow rate of 20 mL/min, a constant current of 25mA and total concentrations less than 200 ppm. A simulated waterwash solution was spiked with concentrated nitrosamines to create approximate nitrosamine concentrations of 50 ppm nitrosopyrrolidine (NPY), nitrosodiethylamine (NDEA) and nitrosomorpholine (NMOR), around 150 ppm total. The removal behavior NPY, NDEA and NMOR during the 12-hour electrolysis period are shown in **Figure 39**. The concentrations of all three nitrosamines reached our LOD within 12 hours and were removed with a 99% removal efficiency. The total charge efficiency during the 12-hour electrolysis period was calculated with the average efficiency during this time at 33%, **Figure 40**. In addition, simultaneous decomposition of the three individual nitrosamines in solution demonstrates no preference to type of nitrosamine, highlighting the robust nature of the cell.

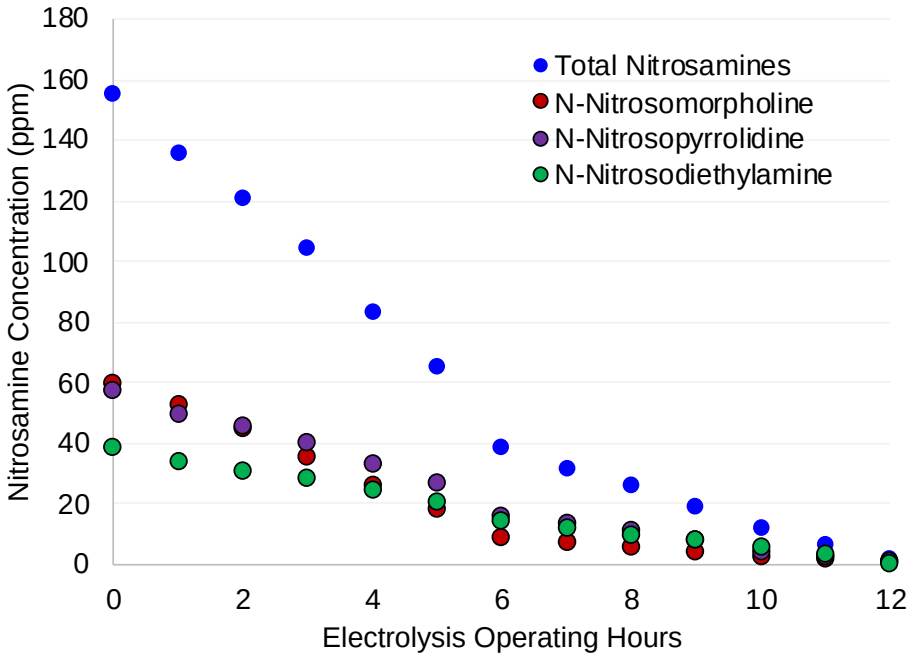

Figure 39. The removal behavior of three nitrosamines using the optimized operating parameters of the flow-through e-cell with simulated waterwash as a function of time

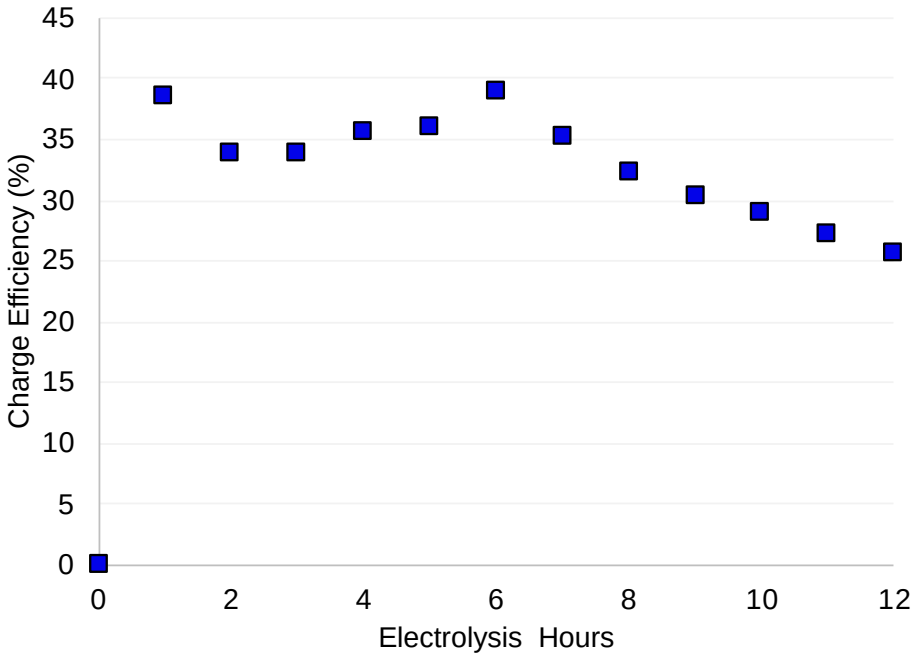

Figure 40. The charge efficiency of three nitrosamines using the optimized operating parameters of the flow-through e-cell with simulated waterwash as a function of time.

3.6.2 Testing of Electrochemical Cell

An authentic waterwash solution was collected from the UK 0.7 MWe small pilot CO_2 capture plant we were able to collect some water wash solution during a recent solvent testing campaign. This water was then used in the flow through e-cell to examine nitrosamine removal. Given no nitrosamines were detected in the water, around 200 ppm nitrosamines were spiked into solution. The results are shown in **Figure 41,** in orange. The performance of the electrochemical cell is maintained when using this authentic waterwash compared to e-cell operation with a simulated waterwash solution (dark blue points, **Figure 41**). The nitrosamine concentrations reached our LOD within 12 hours. This shows that our electrochemical setup can treat nitrosamines from real water wash solutions without any matrix effects.

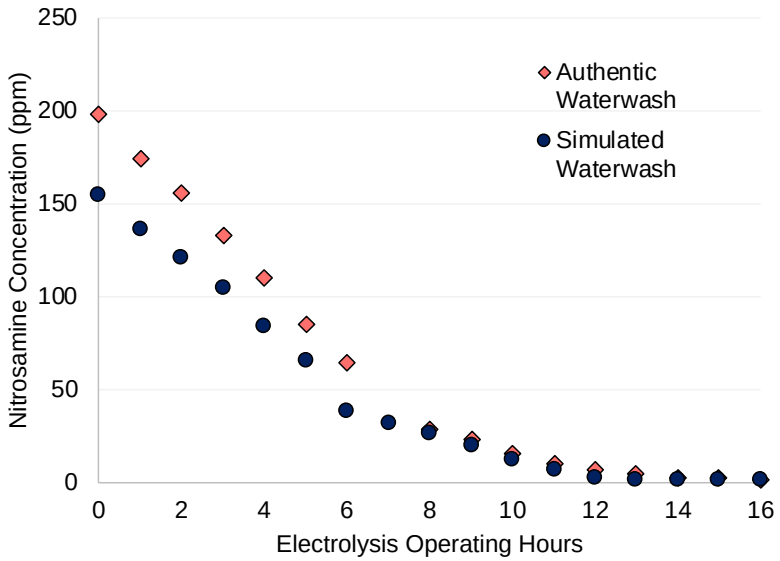

Figure 41. The nitrosamine removal behavior using a flow-through e-cell with authentic waterwash compared to simulated waterwash solution as a function of time.

In addition, the electrochemical reduction does not decompose the matrix of the waterwash solution. The solvent concentration in the water is stable during the 12 hours of electrolysis when nitrosamines were present in solution (**Figure 42**). This indicates that the flow through electrochemical process is beneficial as it does not decompose the solvent in the water wash meaning the solvent can be returned to the solvent loop.

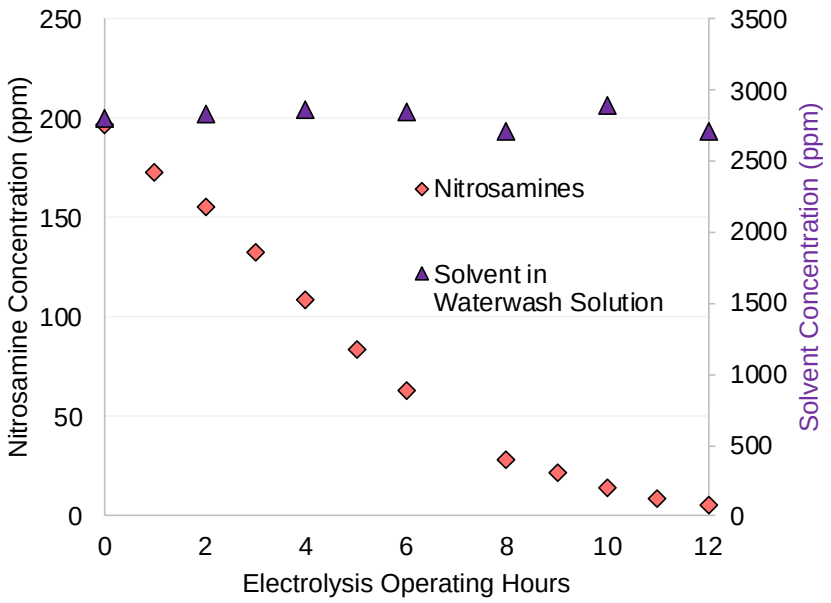

Figure 42. The nitrosamine removal behavior and solvent concentration using a flow-through e-cell with authentic waterwash.

The flow through e-cell was operated for around 500 hours using carbon electrodes to evaluate the long-term stability of the electrodes. The e-cell was operated using repetitive cycles of nitrosamine spike and nitrosamine removal until 500 hours of operation was reached. Every cycle the flow direction was swapped from cathode towards anode to anode towards cathode. The e-cell was operated at a constant current of 25 mA using a 20 mL/min flow rate. The solution volume of 500 mL was maintained throughout each cycle, meaning fresh simulated waterwash solutions was added with each nitrosamine spike. The results are presented in **Figure 43**. Samples were taken periodically throughout the cycles however only the initial and final concentrations are shown. The flow direction did not impact the nitrosamine removal performance as each cycle generally reached the same final concentration level, > 90% nitrosamine removal. This data shows that the nitrosamine removal performance is stable over long term operations and that the carbon electrodes are stable under these operating conditions. SEM images confirm the carbon electrodes exhibited no visible degradation during the 500 hours of operation.

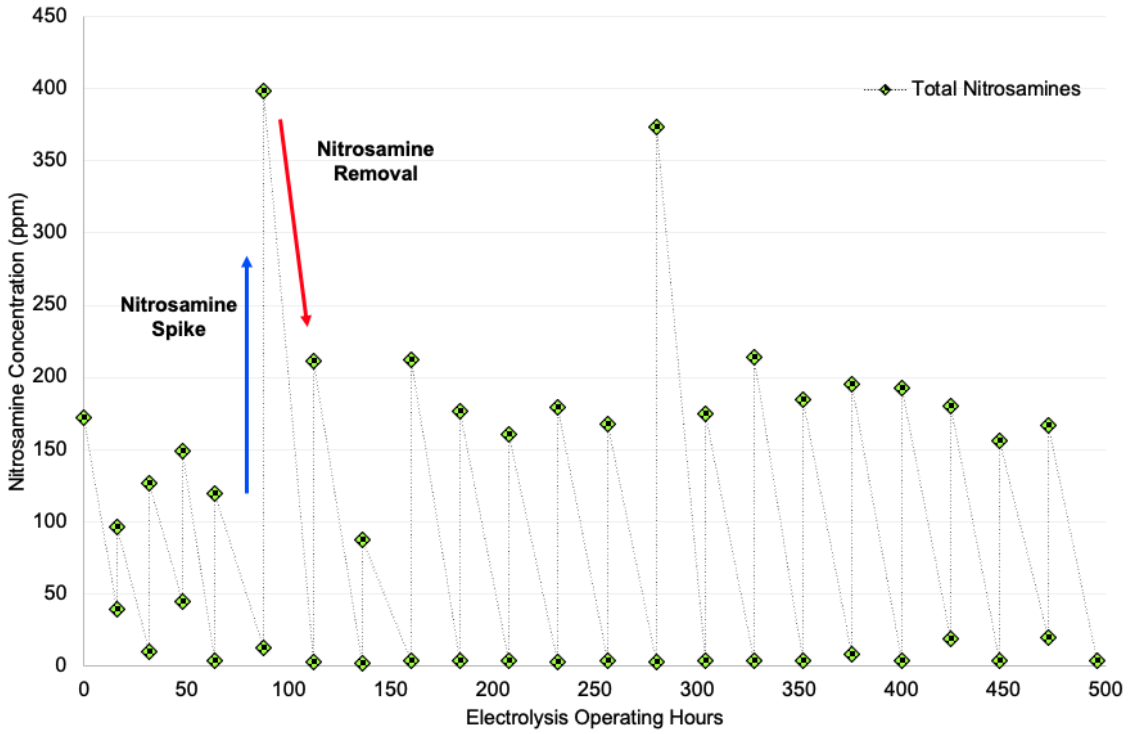

Figure 43. The total nitrosamine removal behavior using flow-through e-cell with Carbon Cloth electrodes over 500 hours of operation.

3.7 Integrated Study with Dynamic Packing and Modified Solvent and Electrochemical Cell (Task 8)

3.7.1 Solvent and Additive Determination

The UK solvent and additive composition were determined during parametric testing and remained constant during the duration of the long-term testing.

3.7.2 Parametric Testing

A total of six different packings including stainless steel packing, ABS packing, nylon packing and three dynamic packings were tested in small bench CO_2 capture unit (**Figure 44**). All the 3D printing packings are in 250Y shape to compare with; (a) Mellapak steel packing, (b) is made of relatively hydrophobic ABS material without a surrounding shell/wall, Nylon (c) internals with an HDPS shell, DP-1 (d), DP-2 (e), and DP-3 (f) packings are all surrounded with hydrophobic HDPS wall while their internals are fabricated in different portion of nylon and HDPS materials to create the co-polymer dynamic surface. DP-1 (d) has a nylon base with a small amount of HDPS horizontal strips in the DP-1 packing interior. DP-2 (e) has alternating pattern interior with 50% HDPS and 50% nylon material, while DP-3 also has a nylon base with a small amount of HDPS embedded with an arrow pattern.

Figure 44. 250Y geometry packing fabricated from different materials; (a) Steel, (b) ABS, (c) Nylon, (d) DP-1, (e) DP-2, (f) DP-3.

The final parametric CO_2 absorption efficiency and solvent loading data are included in the **Figures 45-47** for comparison between all the packing. Both the Nylon and DP-3 packings exhibited improved CO_2 absorption performance when compared to the conventional steel packing. The same CO_2 absorption efficiency can be achieved with higher CO_2 loading in lean return solvent, and the CO_2 loading of rich solvent is shifted to a higher loading region. This translates to a potential reduction of energy demand in the stripper at same CO_2 absorption efficiency.

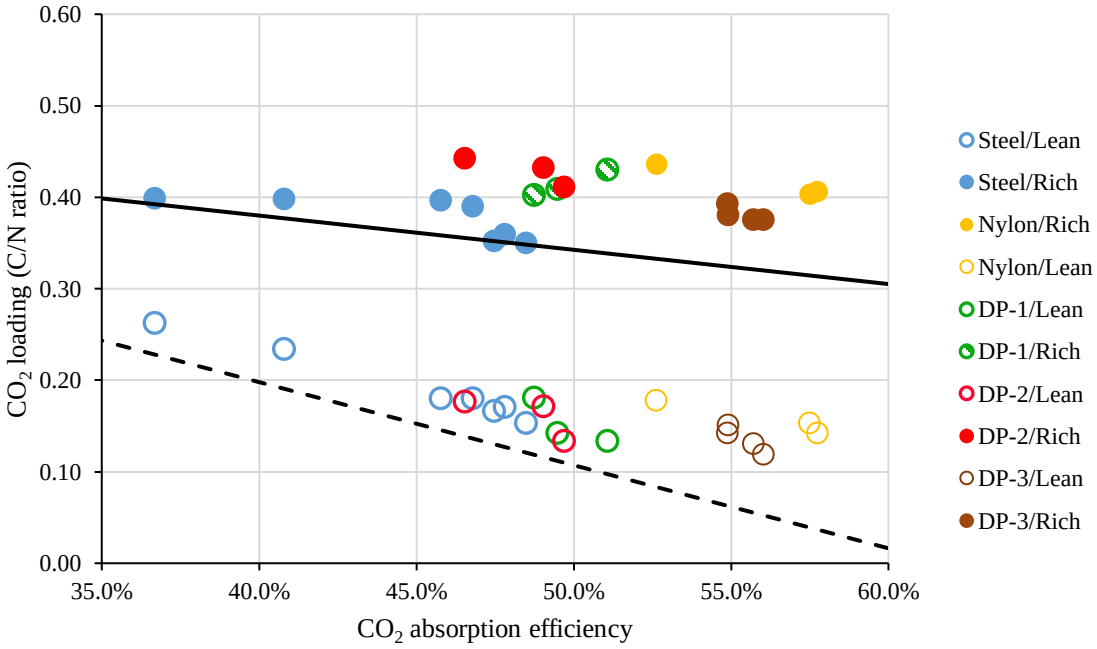

Figure 45. CO_2 absorption efficiency versus lean CO_2 loading at 300 mL/min amine circulation rate. Solid dots: rich CO_2 loading; Open dots: lean CO_2 loading. Solid and dash lines are trendlines for rich and lean CO_2 loading in steel packing cases as baselines.

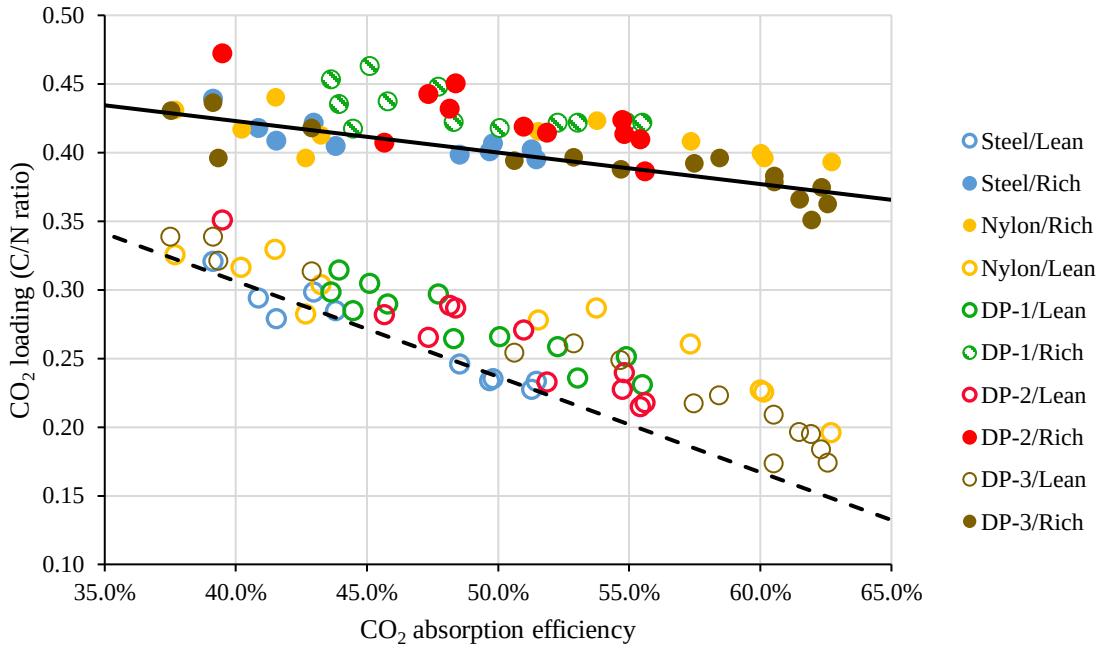

Figure 46. CO_2 absorption efficiency versus lean CO_2 loading at 450 mL/min amine circulation rate. Solid dots: rich CO_2 loading; Open dots: lean CO_2 loading. Solid and dash lines are trendlines for rich and lean CO_2 loading in steel packing cases as baselines.

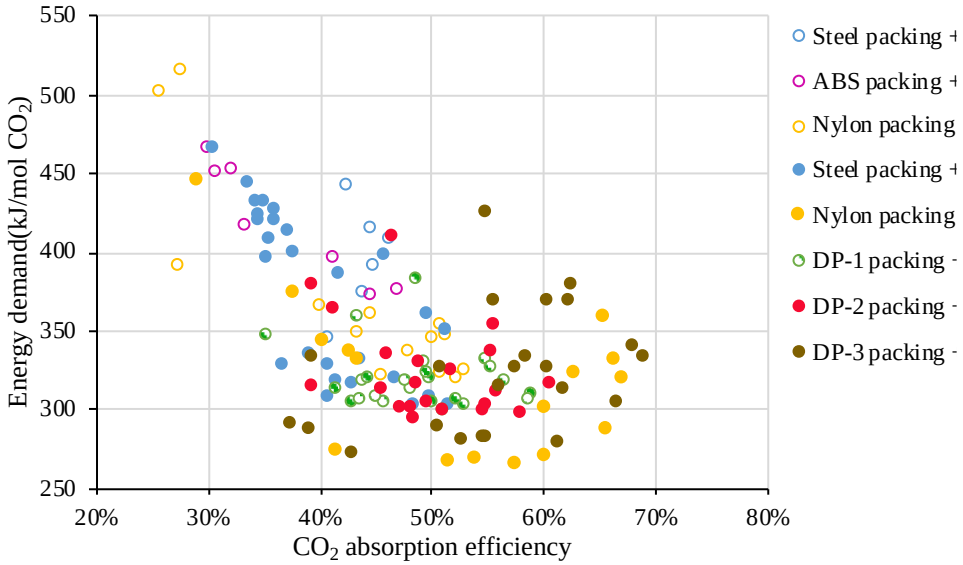

Figure 47. CO_2 absorption efficiency versus lean CO_2 loading at 600 mL/min amine circulation rate. Solid dots: rich CO_2 loading; Open dots: lean CO_2 loading. Solid and dash lines are trendlines for rich and lean CO_2 loading in steel packing cases as baselines.

A summary of the energy demand and CO_2 absorption efficiency of all cases at different operation conditions is shown in **Figure 48.** During the parametric testing, employing the 3D printing packing results in an overall improved CO_2 capture performance and lower regeneration energy when compared to conventional steel packing (blue circles).

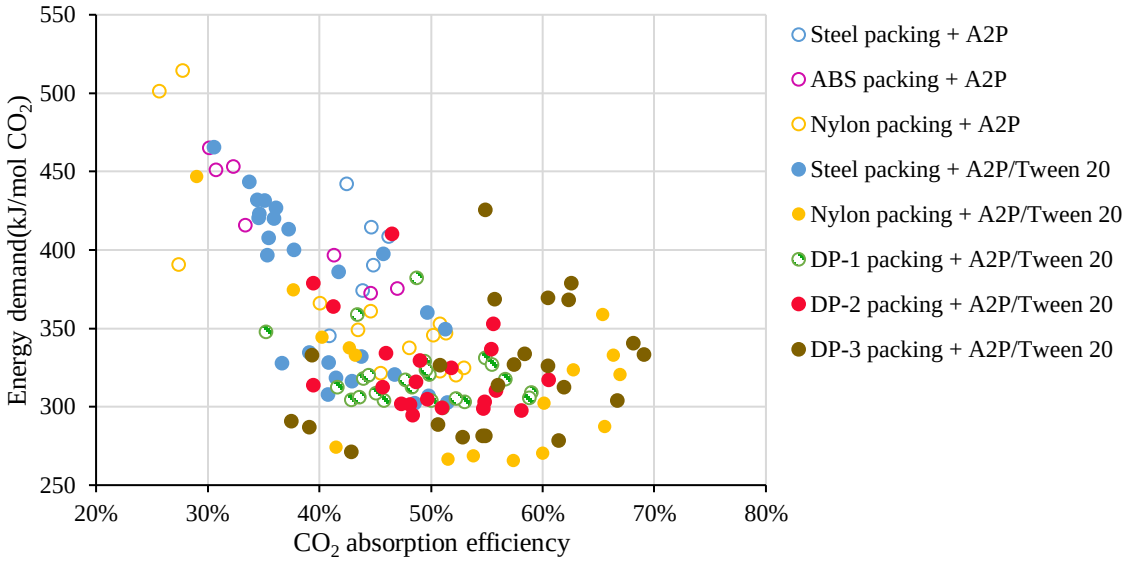

Figure 48. Energy demand versus CO_2 absorption efficiency of all packing tested.

3.7.3 Long-term Testing

The long-term packing verification test consisted of 500 hours of stable CO_2 capture under optimal condition of 450 mL/min amine flow rate and 150 kPa stripper pressure with the DP-3 packing design. The DP-3 packing shows a consistent improvement in mass transfer compared to baseline leading to an average CO_2 absorption of 60.1% and energy demand of 233.8 kJ/mol CO_2 (**Figure 49**). Overall, this translated to a relative 15.9% improvement in CO_2 absorption and 19.7% decrease in energy consumption compared to the system operation with the baseline Mellapak 250Y stainless steel packing.

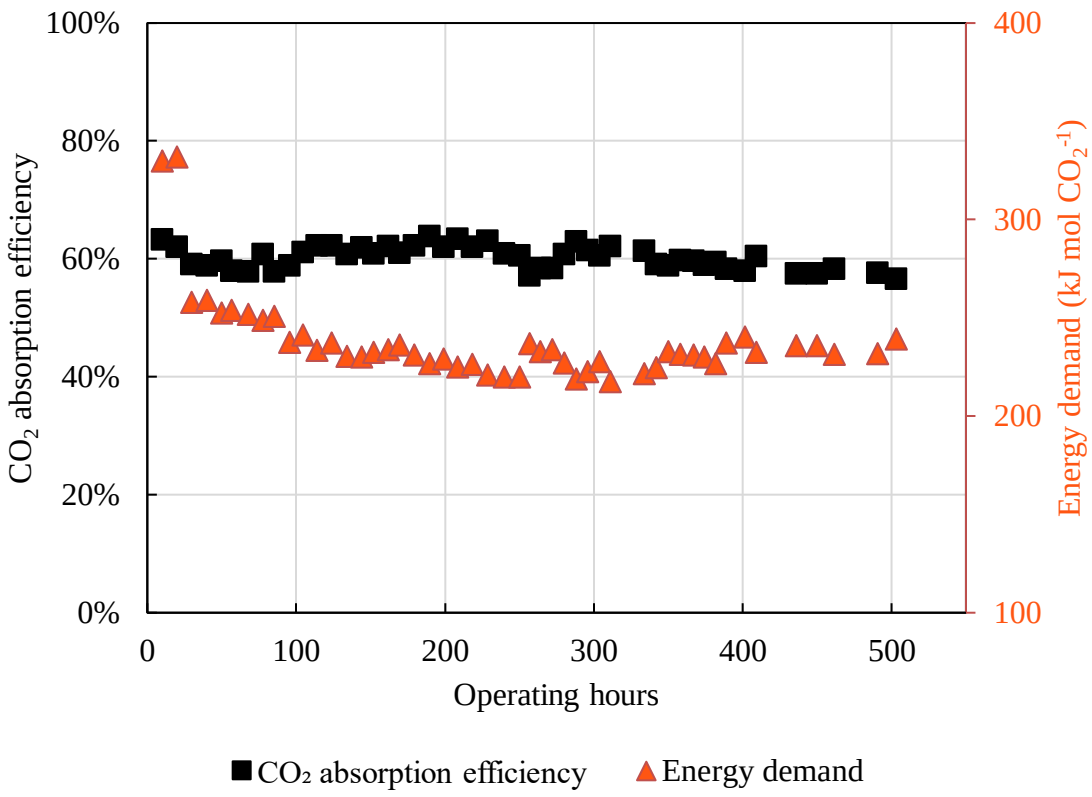

Figure 49. CO_2 absorption efficiency and energy demand during the 500-hour long-term testing (each data point represent a day of testing at stable operating conditions).

The variation of rich and lean solvent alkalinity during the testing period is shown in **Figure 50**. The alkalinity was controlled within 4.5 to 5.5 mol/kg (±10% for 5.0 mol/kg) by balancing water content in inlet and outlet flue gas and with solvent make up when needed. The CO_2 loading in rich and lean solvent is summarized in **Figure 51**. The CO_2 loading in lean solvent is around 0.27 C/N while that in rich solvent is around 0.45 C/N. The dashed lines represent the average values from the comparison operation with steel packing, showing improvement when the steel packing was replaced with the polymer packing.

The CO_2 loading shifted to a higher region when polymer packing is used. In addition, a constant higher cyclic capacity is observed in **Figure 52**. The averaged cyclic capacity in long-term test is 0.84 mol C/kg Solv, which is higher than the 0.76 mol C/kg Solv calculated using the steel packing under the same operating condition.

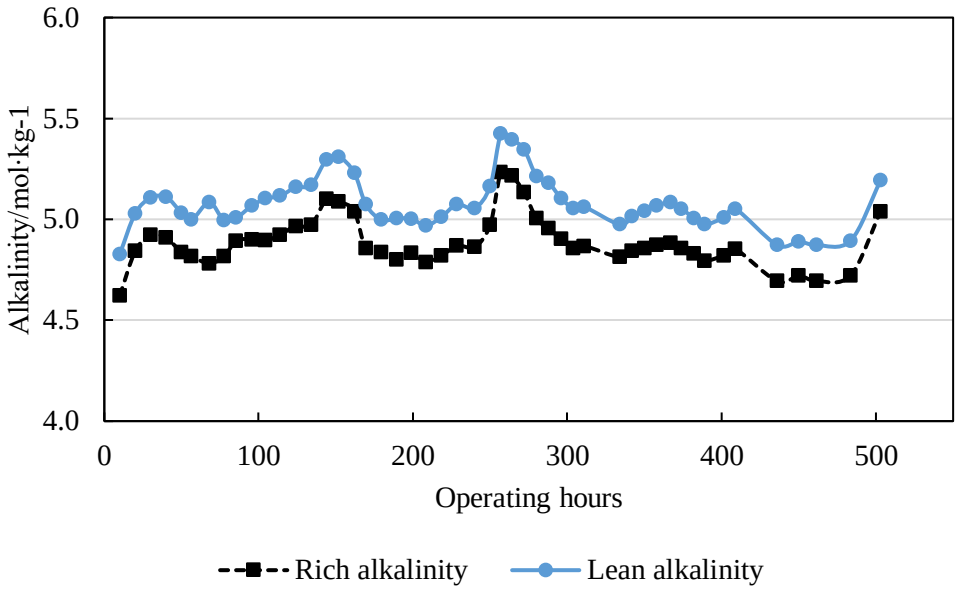

Figure 50. Measured alkalinity of rich and lean solvent

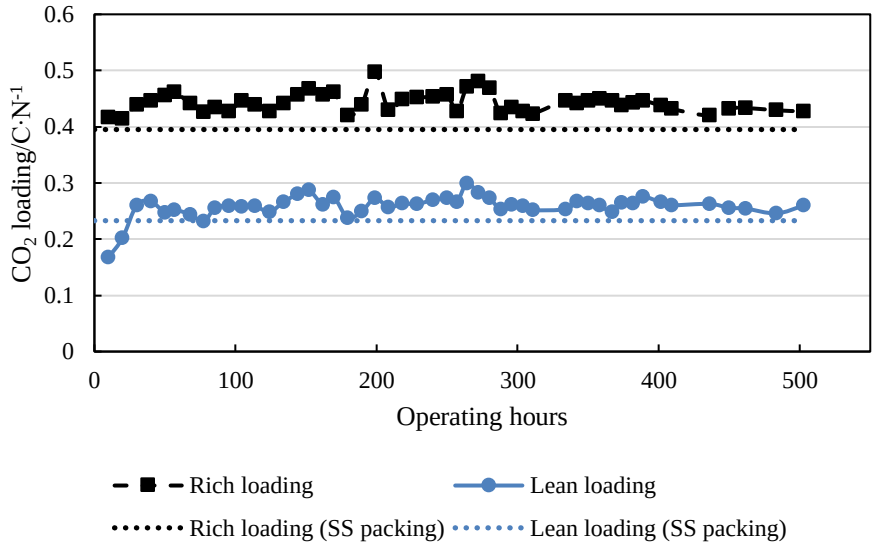

Figure 51. Measured CO_2 loading of rich and lean solvent

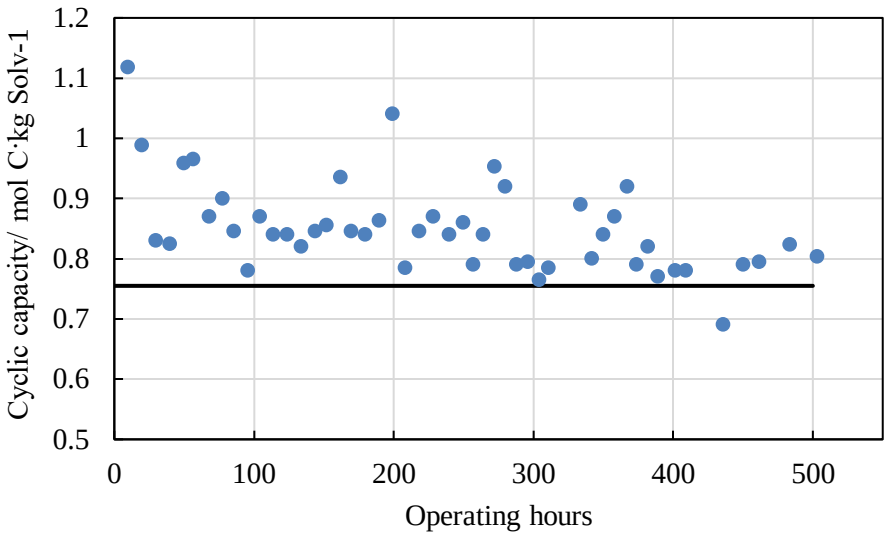

Figure 52. The solvent cyclic capacity during the long-term test where solid line is for SS packing

After the long-term packing verification, the polymer packing showed a consistent improvement in mass transfer leading to an average CO_2 absorption of 60.1% and energy demand of 233.8 kJ/mol CO_2. This improvement translated to a relative 15.9% improvement in CO_2 absorption and 19.7% decrease in energy consumption compared the baseline Mellapak 250Y stainless steel (SS) packing. Given these improvements a more detailed comparison was performed with 72'' SS packing and 48'' dynamic packing in the absorber column (**Figure 53**) to see if the DP packing could achieve the same system performance but with a shorter absorber column. A shorter absorber column will reduce the construction costs which is major factor in the overall cost of CO_2 capture.

The solvent circulation rate for both tests was 450 mL/min to give 2.6 L/G in the absorber and the CO_2 loading in lean solvents ranged from 0.22 to 0.32 C/N. The absorber temperature profile of the dynamic packing indicates a CO_2 absorption enhancement when compared to that of SS packing, as shown in **Figure 54.** Thermocouple 2 measured temperature on the top of both structured packings and thermocouple 6 measured temperature below the SS packing. Given the shorter dynamic packing height, thermocouple 5 was located below the last dynamic packing section. A fast temperature drop is observed when there is insufficient gas-liquid contact. The lean solvent enters the absorber column between thermocouples 1 and 2 with a set temperature of 40 °C. A stronger heat release was observed with dynamic packing where the maximum temperature was 57 °C versus 54 °C with the steel packing due to CO_2 absorption enhancement.

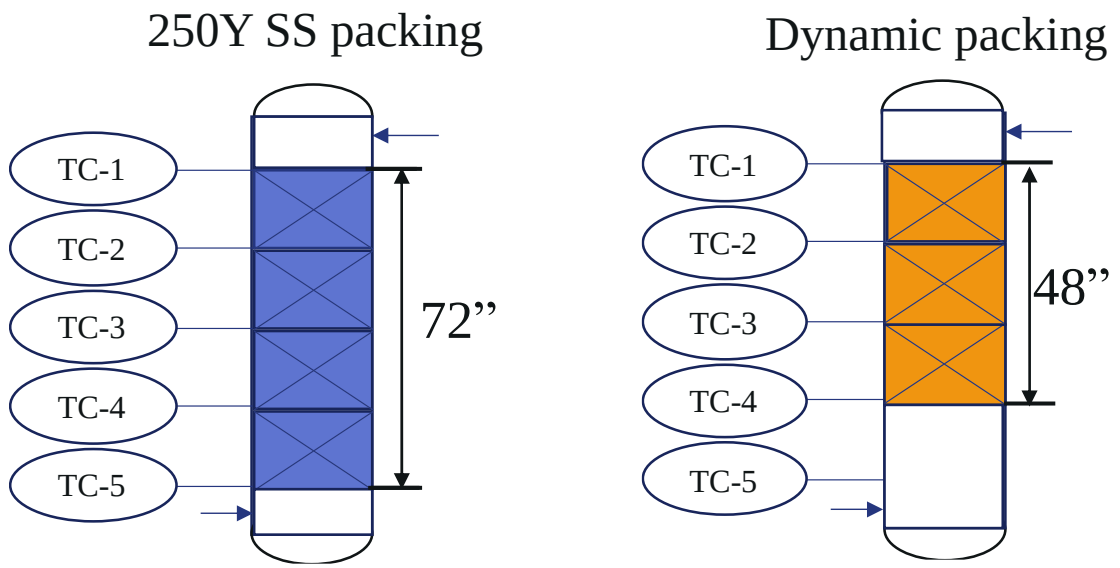

Figure 53. Absorber configuration of baseline Mellapak 250Y stainless steel (SS) packing and dynamic packing to estimate CO_2 adsorption efficiency enhancements.

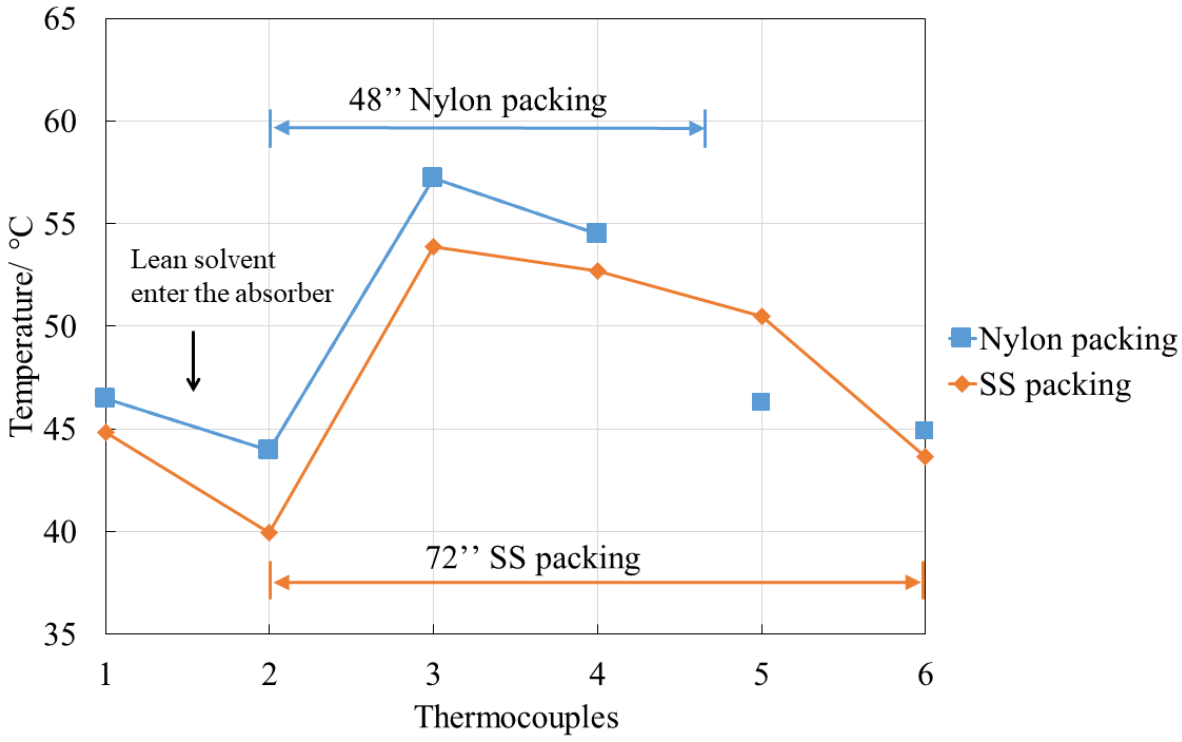

Figure 54. Temperature profile of absorber column with different packing configurations

The CO_2 loading in the lean solvent ranged from 0.22 to 0.32 C/N, resulting in normalized free amine from 4.6 to 7.4 mol/kg gas (**Figure 55**), with the CO_2 loading of the rich solvent falling near the same trendline (**Figure 56**). These two absorber configurations showed similar CO_2 absorption rate and demonstrated that mass transfer in the absorber column was enhanced with the more efficient dynamic packing and can reach the CO_2 removal target with less packing height (66.7% of original height). By reducing the required amount of packing the size of the absorber column and its capital expense can be substantially reduced.

Lastly, the carbon balance between CO_2 removed from gas phase and absorbed in liquid phase is shown in **Figure 57.** The gas phase data was obtained through reading of gas analyzer and liquid phase data was obtained through TIC (total inorganic carbon) measurement. The data presented shows acceptable agreement with an average deviation of 6.5%.

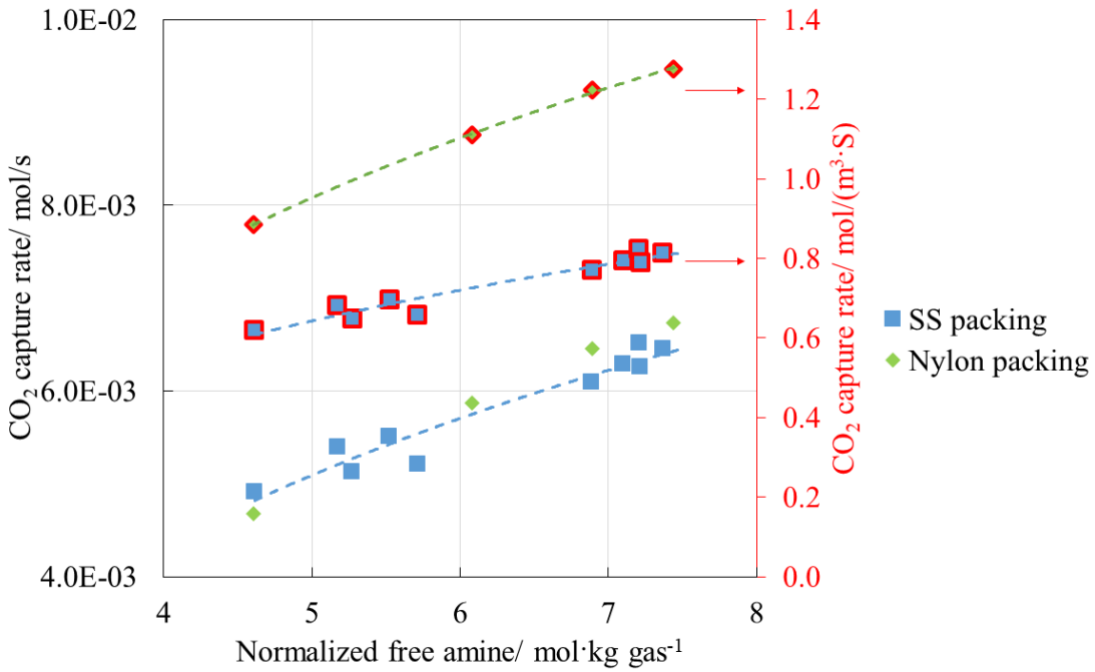

Figure 55. Comparison of the CO_2 absorption rate with different absorber column configurations, the free amine refers to the reactive amine in lean solvents

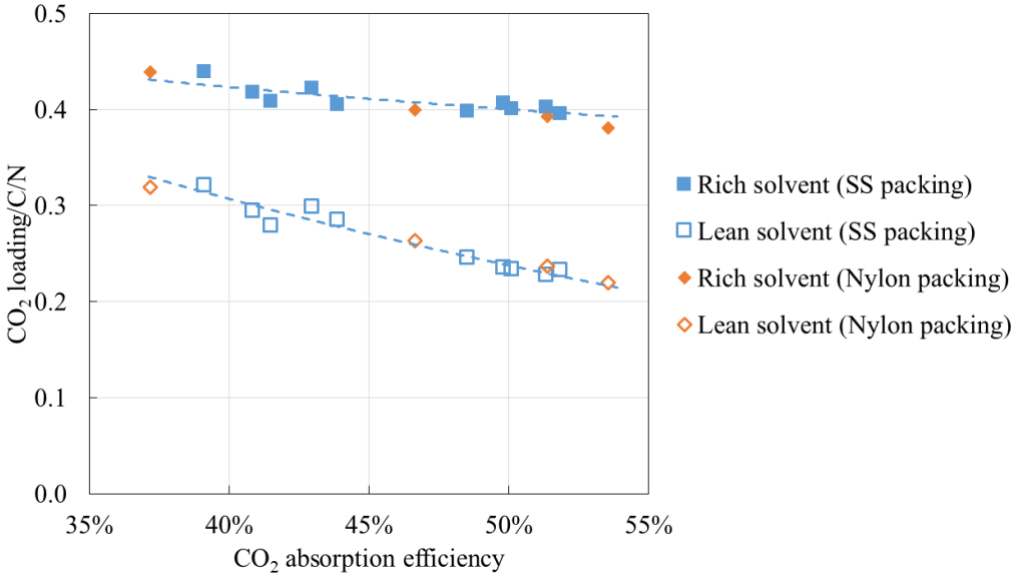

Figure 56. CO_2 loading of lean and rich solvent with different absorber configurations

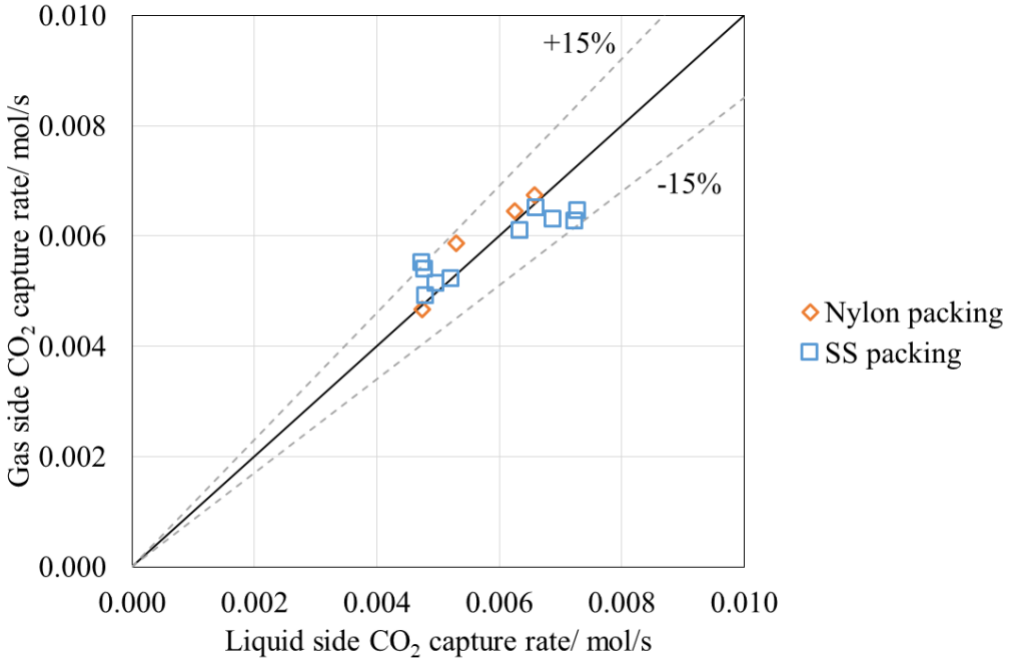

Figure 57. CO_2 balance between gas and liquid phases

3.7.4 Degradation and Aerosols

After the 500-hour testing period was completed a detailed solvent degradation analysis was conducted using a previously identified degradation mechanism for the main amine component in the solvent. The analysis was conducted using LC/MS of the samples collected during the long-term testing period. At the end of the 500-hour testing period, the observed amine degradation totaled 3900 mg/L. The individual degradation products matched with previous testing campaign using the same solvent. The solvent degradation with the polymer packing was then compared to the degradation trends during similar solvent testing campaigns performed at UK CAER 0.7 MWe carbon capture system. This comparison is presented in **Figure 58**. The degradation rate is generally comparable to all the previous solvent tests through the 500-hour mark with no new degradation products identified in the solvent used with the polymeric packing. This suggested that the polymer packing has minimal to no impact on solvent stability.

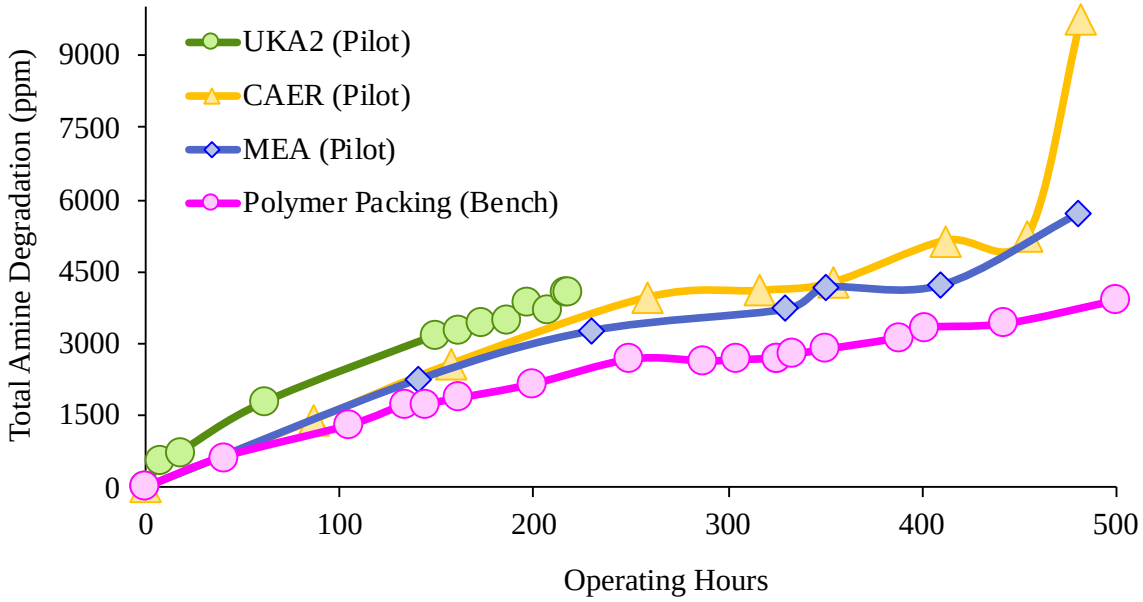

Figure 58. Solvent degradation measured during the SBU long-term campaign compared to other solvent testing campaigns.

3.8 Technical and Economic Analysis (Task 9)

The TEA report summarizes the evaluation of a CO_2 capture technology developed by University of Kentucky (UK) for post-combustion carbon capture. The evaluation uses a TEA report prepared by Trimeric Corporation as the basis for the UK CO_2 capture process with UK amine solvent. A process modification is added here by applying advanced packings in the absorber to enhance mass transfer and decrease the absorber size using the UK amine solvent CO_2 capture system. This assessment assumed that the cost of the absorber packing is the same for steel and the 3D printed polymers with the decrease in capital cost only related to decreasing the size of the absorber and it ancillary impact on the CO_2 capture system. The UK process with advanced packings shows

reduction in levelized cost of electricity (~10.4%), and cost of CO_2 capture (~24.4%). The UK CO_2 capture process with and without advanced packings are compared to Case B12B (CO_2 capture from a supercritical pulverized coal power plant using Shell Cansolv capture technology and solvent) from the Department of Energy (DOE) National Energy Technology Laboratory (NETL) report.

The UK CCS system for fossil fuel generation builds on traditional carbon capture technology with process intensification, heat recovery, balancing the capital and operating costs and with an advanced control strategy. Case B12A (without capture) and Case B12B (capture with Shell CANSOLV®) are the benchmark from the NETL Rev 4 Baseline Report. UK CCS system is escalated based on the stream from a power plant that generates 650 MWe (net) of electricity. The system has three key process modifications: 1) advanced packings are applied to decrease absorber size while achieving same CO_2 removal and solvent rich loading; 2) a secondary stripper is applied to further decrease lean solvent CO_2 loading and send CO_2 enriched air to coal-fired boiler to increase CO_2 partial pressure in flue gas; 3) desuperheat steam extracted for amine regeneration by heat exchange with the boiler feed water. **Figure 59** shows more details on the process advancements and design basis.

The base UK process (UK PCC 1), and with advanced packings (UK PCC 2) shows reduction in levelized cost of electricity and the cost of CO_2 captured. The LCOE decreased by 10.4% (**Figure 60**) in UK PCC 2, and the cost per tonne of CO_2 capture also decreased by 24.4% (**Figure 61**). The $34.49 relative cost per tonne of CO_2 captured is a significant decrease from the reference case and shows a new pathway to the target of $30 tonne. Specifically related to the absorber packing developed in this project, the capital cost decrease contributed to approximately 77% of the reduction in the cost of capture, where the decrease comes from both the deployment of advanced packings and the novel aspects of the UK CO_2 capture process.

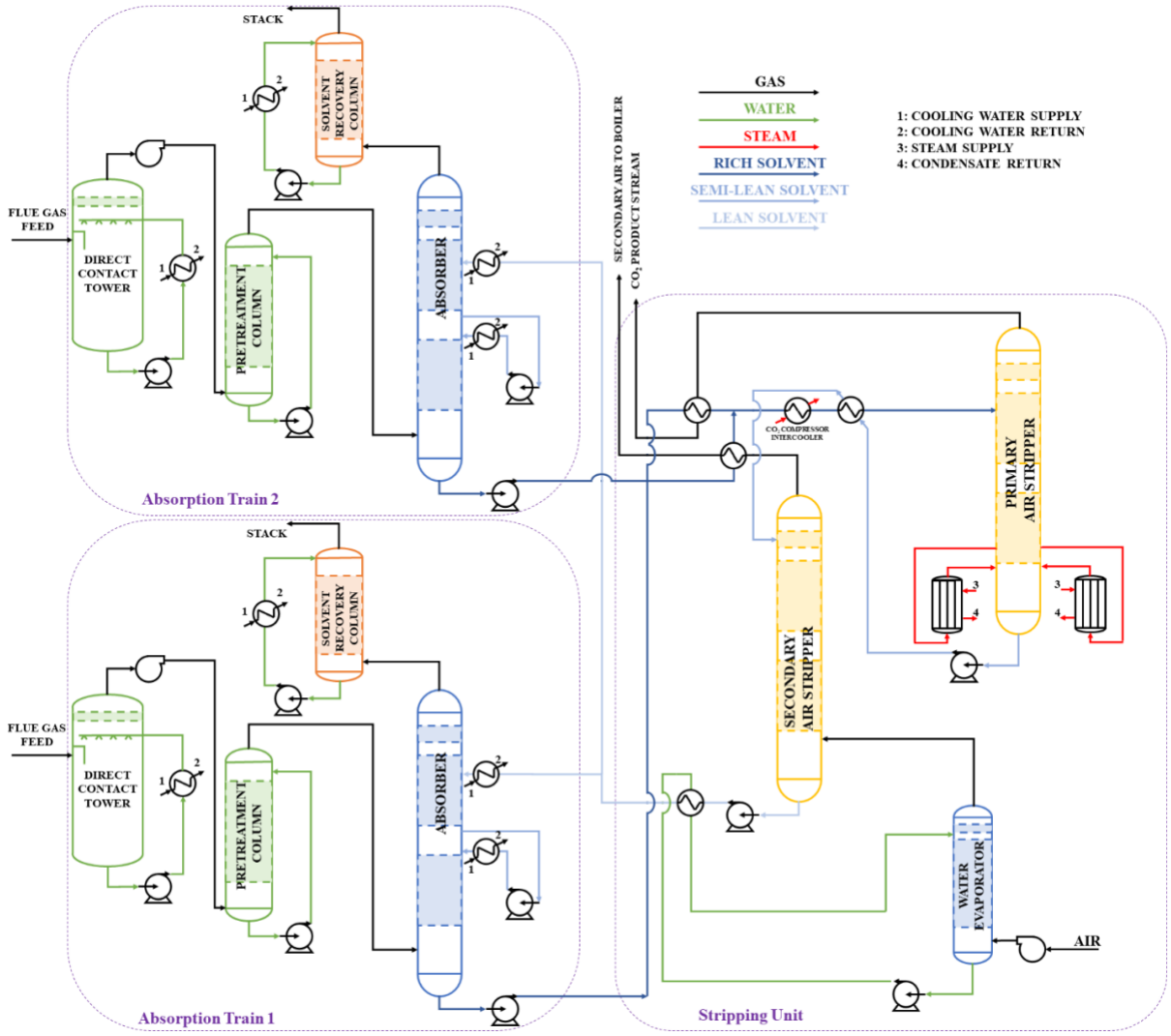

Figure 59. UK CCS Process (UK PCC 1)

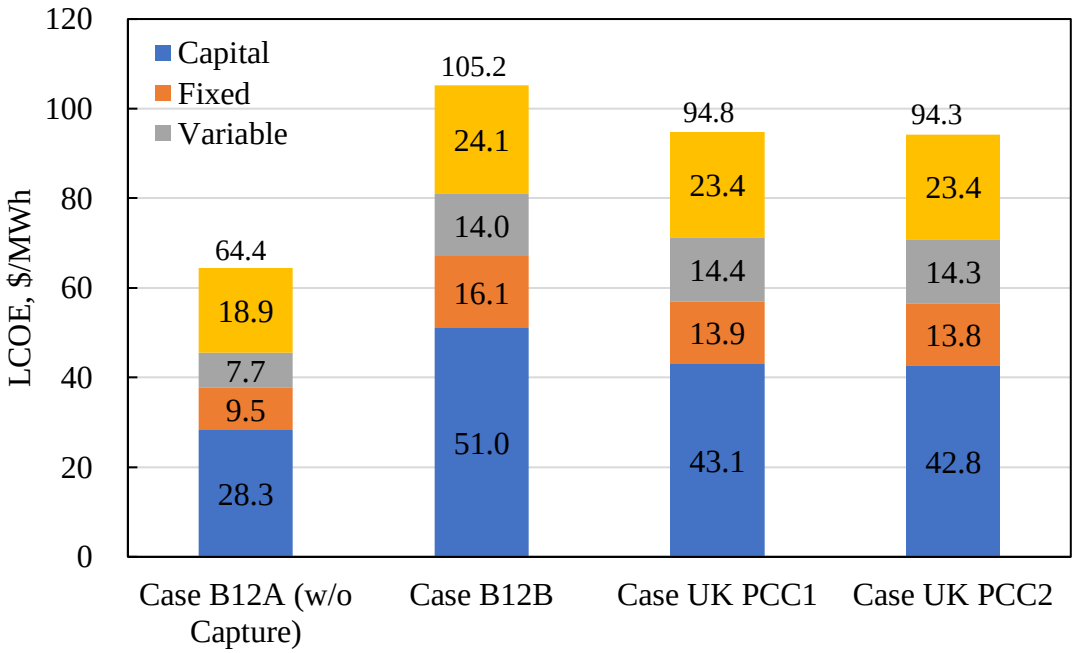

Figure 60. LCOE by Cost Category (TS&M is excluded).

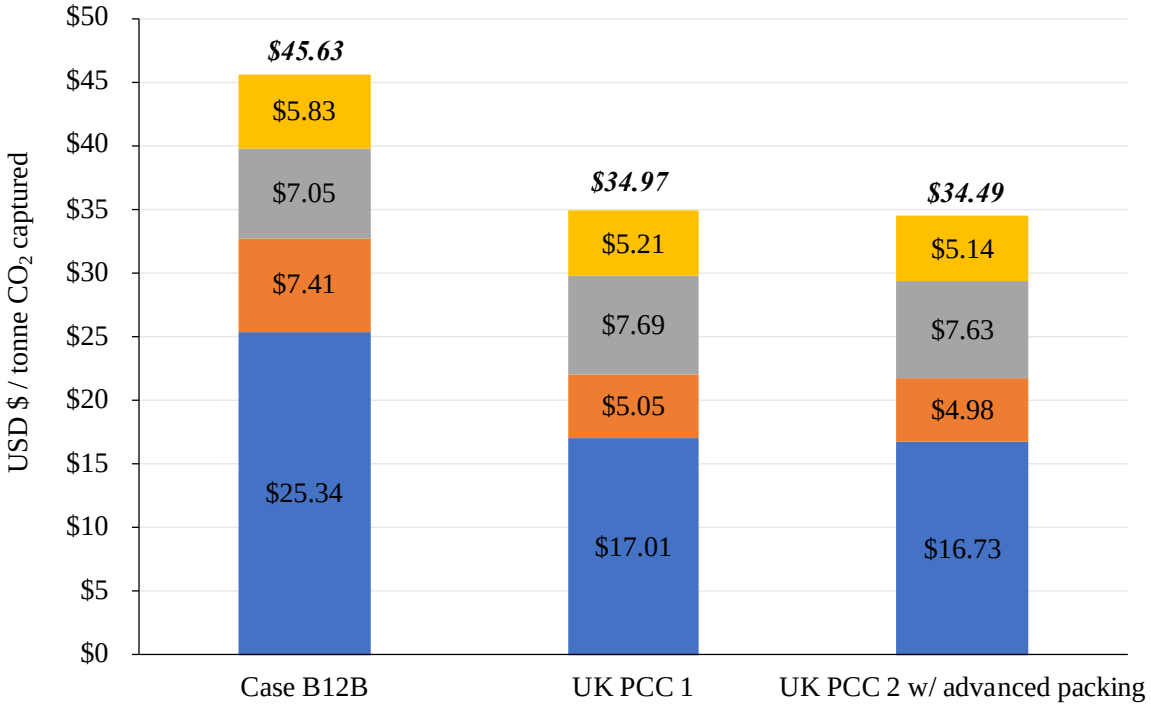

Figure 61. Relative cost per tonne of CO_2 captured compared to reference case.

4.) Appendices

Table A1. Success Criteria Summary

Success Criteria	Percent Complete	Accomplishments
1. (Task 3) Design of the Dynamic Packing: A complete specification and finalized design of dynamic packing	100%	Three polymeric materials (HDPS, ABS, Nylon) showed long-term stability after exposure to CO_2-loaded amine solvent at elevated temperature (60 °C) with minimal changes to contact angle on the polymer surface.
2. (Task 3) Fabrication of the Dynamic Packing: Production of a 4" x 3' section of dynamic packing capable of being integrated into UK bench CO_2 capture unit	100%	Multiple 3" diameter polymeric packing section were printed with multiple polymer configurations and installed in the UK small bench CCS. Baseline testing showed comparable CO_2 capture efficiency and rich solvent loading compared to conventional steel packing.
3. (Task 4) A completed test matrix plan for the dynamic packing and solvent test campaign to achieve the program objectives	100%	UK solvent and additives were selected and obtained in sufficient quantities. Process variables relevant to the bench unit operation were identified.
4. (Task 5) Printing and Testing of Dynamic Packing; A completed test campaign for the dynamic packing to achieve the target 20% mass transfer enhancement	100%	Process variables relevant to the bench unit operation were identified. Baseline testing showed comparable CO_2 capture efficiency and rich solvent loading compared to conventional steel packing.
5. (Task 7) Electrochemical Cell Design, Fabrication and Testing: Production of a electrochemical cell capable of decomposing nitrosamines below the target value of 60% removal	100%	Electrochemical cell was shown to decompose greater than 90% of nitrosamines from a simulated waterwash with a charge efficiency above 15%.
6. (Task 8) Packing Parametric study: The recommended optimized system operating parameters need to achieve a 20% increase in mass transfer.	100%	Parametric testing was completed with 4 different dynamic packing designs and showed a >20% increase in CO_2 mass transfer.
7. (Task 8) Packing Long-term verification tests: A stable operation with average of 90% CO_2 capture (equivalent) with average of 20-30%	100%	Long-term testing with 500 hrs. completed.

less energy consumption compared to the MEA reference.		
8. (Task 9) TEA: The completed high level technical and economic analysis of the proposed process concepts for a 550 MW power plant that shows a pathway to achieving carbon capture up to 90% with a less than \$30/tonne CO_2 captured according to the DOE guidelines.	100%	The UK process with advanced packings shows a cost of \$34.49/tonne CO_2 captured, a 24.4% reduction from Case B12B.

Table A2. Project Milestones

Budget Period	ID	Task Number	Title	Description	Planned Completion Date	Actual Completion Date	Verification Method
1	A	1	Updated Project Management Plan	The Project Management Plan was revised after the project award to reflect changes during project initiation; revised to modify milestones and revised schedule.	10/31/2018	10/12/18 2/6/2019 4/6/2020 4/30/2020	Revised PMP Revision A Revised PMP Revision B Revised PMP Revision C Revised PMP Revision D
1	B	1	Kickoff Meeting	Web-based presentation given to DOE and NETL Project Managers	11/15/2018	11/27/18	Presentation file
1	C	1	Subcontracts Established	Subcontract with LLNL	1/31/2019	1/10/2019	Written Verification
1	D	2	Solvent Physical Properties	Identification of amine solvent additive that can deviate surface tension by up to 20%	6/30/2019	6/28/2019	Quarterly report
1	E	3	Dynamic Packing Material Development	Polymeric material(s) selected for 3D-printing that shows longer-term (1000+ hour) stability in amine solvents as measured by mass loss and deformation	6/30/2019	6/28/2019	Quarterly report
1	F	3	Documented Packing Fabrication Complete	Fabrication of a 3" x 3" 3D-printed dynamic packing section with contact angle differences of ≥10° and increasing CO_2 mass transfer by 10-20% compared to reference	3/31/2020	3/6/2020	Quarterly Report
1	G	5	Baseline Solvent Testing Complete	Small bench solvent testing showing a ≥10% decrease in regeneration energy compared to reference	3/31/2020	3/6/2020	Quarterly Report
1	H	7	Nitrosamine Electrochemical Cell	Faradic efficiency of electrochemical cell at >10% with nitrosamine simulated waterwash solution	9/30/2019	9/30/2019	Quarterly Report
1	I	7	Nitrosamine Electrochemical Cell	Electrochemical cell capable of achieving a removal efficiency of 60%	3/31/2020	9/30/2019	Quarterly Report
2	J	7	Nitrosamine Electrochemical Cell	Electrochemical cell efficiency of 20% with nitrosamine spiked simulated waterwash solution	6/30/2021	9/30/2021	Quarterly Report
2	K	8	Integrated Solvent/Packing Testing Complete	Integrated Solvent/Packing Testing showing an increase in CO2 capacity (C/N) and reducing the liquid circulation by 10% compared to reference	6/30/2022	6/30/2022	Quarterly Report
2	L	9	Issue Technical Report on TEA	High level technical and economic assessment	6/30/2022	6/30/2022	Technical Report appended to Quarterly Report

Table A3: Project Output

Title	Location	OSTI/Link
Oral Presentations		
Decomposition of nitrosamines through electrochemically mediated reduction on carbon xerogel electrode.	ACS Spring 2019 National Meeting & Exposition, Orlando FL, March 31 – April 4, 2019	https://doi.org/10.2172/1733231
Advancing Post-Combustion CO_2 Capture through Increased Mass Transfer and Lower Degradation	2019 Carbon Capture, Utilization, Storage, and Oil and Gas Technologies Integrated Review Meeting, Pittsburgh, PA, August 26-30, 2019	https://netl.doe.gov/sites/default/files/netl-file/J-Thompson-UKY-CAER-Increased-Mass-Transfer.pdf
Modifying Amine Solvent Properties to Increase CO_2 Mass Transfer	5th Post Combustion Carbon Capture Conference (PCCC5), 17th-19th September 2019, Kyoto Japan	https://doi.org/10.2172/1763066
Effect of changes of physical properties on CO_2 capture solvents on its absorption rate	ACS Fall 2020 National Virtual Meeting, August 17 - 20, 2020	https://doi.org/10.2172/1732159
Journal Papers		
Research on oxygen solubility in aqueous amine solvents with common additives used for CO_2 chemical absorption	International Journal of Greenhouse Gas Control, 2022, 116, 103646	https://doi.org/10.1016/j.ijggc.2022.103646
CO_2 absorption intensification using three-dimensional printed dynamic polarity packing in a bench-scale integrated CO_2 capture system	AIChE J. 2022, e17570	https://doi.org/10.1002/aic.17570
Efficient carbon capture using sub-textured polymer packing surfaces via 3D printing	Chemical Engineering Science 267 (2022) 118320	https://doi.org/10.1016/j.ces.2022.118320
Matching CO_2 capture solvents with 3D-printed polymeric packing to enhance absorber performance	Proceedings of the 15th Greenhouse Gas Control Technologies Conference 15-18 March 2021	https://papers.ssrn.com/sol3/papers.cfm?abstract_id=3814402

Mass transfer intensification through increased surface wetting and liquid turbulence using 3D printing structured packing for CO_2 capture	Proceedings of the 16th Greenhouse Gas Control Technologies Conference (GHGT-16) 23-24 Oct 2022	https://papers.ssrn.com/sol3/papers.cfm?abstract_id=4274369
Oxygen Solubility in Aqueous Amine Solvents with Common Additives Used for CO2 Chemical Absorption	Proceedings of the 16th Greenhouse Gas Control Technologies Conference (GHGT-16) 23-24 Oct 2022	https://papers.ssrn.com/sol3/papers.cfm?abstract_id=4274367
NETL Review Meeting Presentations		
Advancing Post-Combustion CO_2 Capture through Increased Mass Transfer and Lower Degradation	2022 Carbon Management Project Review Meeting - Point Source Carbon Capture, Pittsburgh PA, August 15-19, 2022	https://netl.doe.gov/sites/default/files/netl-file/22CM_PSC19_Thompson.pdf
Advancing Post-Combustion CO_2 Capture through Increased Mass Transfer and Lower Degradation	National Energy Technology Laboratory Carbon Management and Natural Gas & Oil Research Project Review Meeting Virtual Meetings, August 2-31, 2021	https://netl.doe.gov/sites/default/files/netl-file/21CMOG_PSC_Thompson.pdf
Advancing Post-Combustion CO_2 Capture through Increased Mass Transfer and Lower Degradation	2019 Carbon Capture, Utilization, Storage, and Oil and Gas Technologies Integrated Review Meeting - Capture and Utilization Sessions. Pittsburgh PA, August 26-30, 2019	https://netl.doe.gov/sites/default/files/netl-file/J-Thompson-UKY-CAER-Increased-Mass-Transfer.pdf
Advancing Post-Combustion CO_2 Capture through Increased Mass Transfer and Lower Degradation	2018 NETL CO2 Capture Technology Project Review Meeting. Pittsburgh PA, August 13-17, 2018	https://netl.doe.gov/sites/default/files/netl-file/J-Thompson-UKRF-Advancing-Post-Combustion-Capture.pdf